scientific reports

Check for updates

OPEN

Sulfur-mediated transformation, export and mineral complexation of organic and inorganic C, N, P and Si in dryland soils

Xin Gao[1,2,3], Jie Zhang[2,3], Khan M. G. Mostofa[2,3]✉, Wang Zheng[2,3], Cong-Qiang Liu[2,3], Nicola Senesi[4], Giorgio S. Senesi[5], Davide Vione[6,7], Jie Yuan[8], Yu Liu[2,3], Mohammad Mohinuzzaman[2,9], Longlong Li[2] & Si-Liang Li[2,3]✉

The transformation characteristics of mineral-associated soil components have profound impacts on their physical, biological, and chemical properties in drying-affected soils, whereas their mechanisms of sequestration and transformation remain elusive. To elucidate these phenomena, the solid-phase, water extracts (labile state, LS) and alkali-extracts (complexed state, CS) of four drying-affected soil types were examined. On average, the contents of soil organic carbon (SOC), soil total nitrogen (STN), and soil total hydrogen (STH) decreased in the order: forest > grassland > agriculture > desert. The extracted dissolved organic matter $(DOM)_{LS}$, DOM_{CS} and nutrients varied greatly among soil types, which indicated the occurrence of mineralization, sequestration, neoformation, and either export or emission. In particular, the relatively high levels of dissolved inorganic carbon $(DIC)_{LS}$ and relatively low levels of DIC_{CS} in agricultural soils could be ascribed to the impact of human activities, i.e., tilling and cultivation, on mineral-bound DIC, leading to its export in LS forms. The stable isotopes of $\delta^{13}C$-SOC and their significant relationships with DIC_{LS} and $SO_4^{2-}{}_{LS+CS}$ suggest the occurrence of carbon and sulfur sequestration through the uptake of CO_2, DIC, or carbonyl sulfide (COS) following their generation from SOC or DOM mineralization. In forested and agricultural soils, the humic substances (HS) components in LS forms were subjected to a substantial degradation, whereas HS_{CS} components remained mostly unaffected, implying their occurrence in organo-mineral protection. Overall, low soil total sulfur (STS) and sulfate $(SO_4^{2-})_{LS+CS}$ contents were correlated with high amounts of soil components in both the solid and liquid phases, and vice versa. These findings suggest that microbial SO_4^{2-} might operate in the dissolution and mineralization of HS-bound organo-minerals, which would potentially generate soil inorganic carbon (SIC) or DIC, leading to either their subsequent sequestration as carbonate minerals or their exports and emissions as DIC and CO_2.

Keywords Drying-affected soils, Soil biogenic components, Humic substances, $\delta^{13}C$-SOC, Sulfate reduction, Nutrients

Abbreviations

LS	Labile state, i.e. water extracted fractions (W_e)
CS	Complexed state, i.e. alkali extracted fractions (A_e)
DOC	Dissolved organic carbon. Definition: 'DOC refers to the total amount of dissolved carbon

[1]Key Laboratory of Industrial Ecology and Environmental Engineering (Ministry of Education, China), School of Environmental Science and Technology, Dalian University of Technology, Dalian 116024, China. [2]School of Earth System Science, Tianjin University, 92 Weijin Road, Tianjin 300072, China. [3]Tianjin Key Laboratory of Earth Critical Zone Science and Sustainable Development in Bohai Rim, Tianjin University, Tianjin, China. [4]Dip.to di Scienze del Suolo, della Pianta e degli Alimenti, Università degli Studi di Bari "Aldo Moro", Via G. Amendola 165/A, 70126 Bari, Italy. [5]CNR - Istituto per la Scienza e Tecnologia dei Plasmi (ISTP) - Sede di Bari, Via Amendola, 122, 70126 Bari, Italy. [6]Dipartimento di Chimica, Università degli Studi di Torino, Via P. Giuria 5, 10125 Torino, Italy. [7]Centro Interdipartimentale NatRisk, Via Leonardo da Vinci 44, 10095 Grugliasco (TO), Italy. [8]College of Resources and Environment, Xingtai University, Quanbei East Road 88, Qiaodong District, Xingtai City, Hebei Province, China. [9]Department of Environmental Science and Disaster Management, Noakhali Science and Technology University, Noakhali, Bangladesh. ✉email: mostofa@tju.edu.cn; siliang.li@tju.edu.cn

	found in dissolved organic matter (DOM), which is measured using a total organic carbon (TOC) analyzer'.
DOC_{LS}	LS DOC. Definition: DOC_{LS} refers to the fraction of soil organic carbon (SOC) that is soluble in water extraction from a specific soil.
DOC_{CS}	CS DOC. Definition: DOC_{CS} refers to the fraction of SOC that is insoluble in water extraction but soluble in alkali extraction from the same soil residue after water extraction.
DOC_{LS+CS}	LS and CS DOC
DOM	Dissolved organic matter. Dissolved organic matter. Definition: 'DOM consists of various allochthonous and autochthonous organic substances, primarily composed of distinct functional groups with aliphatic and aromatic structures. These substances contain several important elements, including carbon (C), hydrogen (H), oxygen (O), nitrogen (N), sulfur (S), and phosphorus (P)
LDHs	Layered double hydroxides
$SO_4^{2-}{}_{LS+CS}$	LS and CS SO_4^{2-}
HS	Humic substances
HS_{LS+CS}	LS and CS HS
HA	Humic acids
HA_{LS+CS}	LS and CS HA
FA	Fulvic acids
FA_{LS+CS}	LS and CS FA
PLS	Protein-like substances
PLS_{LS+CS}	LS and CS PLS
SOC	Soil organic carbon
STH	Soil total hydrogen
STN	Soil total nitrogen
STS	Soil total sulfur

Drying-affected soils cover about 40% of the Earth's land surface and undergo multiple climatic stresses such as: low and seasonally variable precipitation, intense solar radiation, high evapotranspiration as well as, depending on the geographical area, relatively short summers and long winters with intense cold weather depending on the geographical area. These factors cause the occurrence of scarce biota and only allow for moderate photosynthesis Schlesinger. Although these conditions result in low soil respiration due to the low soil moisture, dryland soils account for approximately 40% of the global net primary productivity[1].

Furthermore, these conditions increase the risks of desertification, salinization, land degradation, and eolian/water erosion with a strong impact on carbon (C) (including reduced sequestration), nitrogen (N), sulfur (S), phosphorus (P), and silicn (Si) cycles[2–8]. In particular, repeated drying-wetting cycles have a great impact on C, N, S, P, and Si cycling in drylands with consequent possible alteration of their conditions and vegetation decline under changing climate[9–12]. Oxygenic/anoxygenic photosynthesis is reported to take place in soils typically *via* simultaneous C and S sequestration (e.g. carbonyl sulfide, COS, uptake) by soil microorganisms[13–18]. However, the overall dynamics of sequestration of these biogenic components (C, N, S, P, and Si) and their subsequent mineral neoformation remain unclear in diverse soils.

On a global scale, the storage of soil organic carbon (SOC) and soil inorganic carbon (SIC) within 1-m soil depth amounts to approximately 1200–1600 and 695–940 Pg, respectively[19]. Interestingly, most SIC is stored in dryland soils[19,20], thus these soils are effective sites for carbon sequestration via carbonate formation[7,21–23]. Furthermore, the dissolved humic substance (HS) fractions of SOC consistently serve as important reactants in the environment and are directly linked to C cycle in the global ecosystem. Drylands and particularly saline-alkaline soils are usually very rich in sulfate (SO_4^{2-})[24–27], and microbial SO_4^{2-} reduction[28–30] primarily controls the dissolution and mineralization of clay, Fe and layered double hydroxides (LDHs)-like minerals[31,32]. However, in this perspective an integrated understanding of the transformation mechanisms of organic and inorganic C, N, P, Si, S, and HS components in diverse soils is still elusive.

Microbial mineralization of soil components primarily occurs at the mineral-microbes/organic interface[31,32], with labile state (LS) components representing the degradative byproducts under environmental conditions, as they are unable to the neoformation of organo-minerals, so being exported to the surrounding environments. However, some key degradative byproducts are capable of forming organo-mineral complexes that remain in the complexed state (CS) in soil[33,34]. But the mechanisms of generation of LS and CS soil biogenic components under environmental conditions, their possible correlation and the pivotal role played in exporting/emitting and complexing organo-minerals remains unclear.

The aim of this study was thus to clarify: (i) An integrated evaluation of biogeochemical properties for solid phase components (SOC, SIC, STN, STS, STH), labile state (LS) water-extracted components (DOC_{LS}, HS_{LS}, $NO_3^-{}_{LS}$, $NH_4^+{}_{LS}$, $NO_2^-{}_{LS}$, $PO_4^{3-}{}_{LS}$, $SiO_3^{2-}{}_{LS}$ and $SO_4^{2-}{}_{LS}$), as well as complexed state (CS) alkali-extracted components (DOC_{CS}, HS_{CS}, $NO_3^-{}_{CS}$, $NH_4^+{}_{CS}$, $NO_2^-{}_{CS}$, $PO_4^{3-}{}_{CS}$, $SiO_3^{2-}{}_{CS}$, and $SO_4^{2-}{}_{CS}$) of four dryland soil types (forest, agriculture, grassland, and desert) in the Xinjiang Uyghur Autonomous Region that is the most important arid area in China. (ii) A comprehensive study of the biogeochemical sources, neoformation and organo-mineral state of the LS and CS HS components such as humic acids (HA), fulvic acids (FA), and protein-like substances (PLS) in diverse drying-affected soils. (iii) The assessment of SO_4^{2-}-mediated transformation mechanisms of soil components in both solid-phase and liquid-phase LS and CS forms, the sequestration of photosynthetically-derived C and S, organo-mineral neoformation and C protection, as well as corresponding exports or emissions.

Results

Biogeochemical cycling of soil organic and inorganic C with evidence from δ^{13}C-SOC

On average, the highest SOC content was measured in forest soils (51.6 ± 42.0 g/kg) followed by grassland soils (15.6 ± 20.4 g/kg), then agricultural soils (13.8 ± 10.4 g/kg), and desert soils (1.21 ± 0.340 g/kg) (Table 1). This indicates that forest soils can store SOC arising from the repeated input of plant materials, and that soils covered by dense forests are relatively unaffected by drying effects. The SOC contribution to soil total carbon (STC), on average, followed the order: forest (66.7 ± 20.0%) > agriculture (43.7 ± 25.7%) > grassland (41.6 ± 29.0%) > desert (15.0 ± 8.4%).

On average, the SIC content was the highest in forest soils (16.9 ± 10.0 g/kg) and it was approximately 27.0%, 42.0%, and 111.0% higher compared to, respectively, grassland, agricultural, and desert soils. This finding suggests that all soil types contribute to SIC storage and sequestration in drying-affected or arid regions. Interestingly, not only the SOC content was substantially higher in forest soils than in grassland, agricultural, and desert soils (230%, 275% and 4159%, respectively), but the SIC content was also relatively higher in forest soils than that in the other three soil types. However, the average contribution of SIC to STC followed the order: desert (85.0 ± 8.4%) > grassland (58.4 ± 29.0%) > agriculture (56.3 ± 25.7%) > forest (33.3 ± 20.0%), with the highest level in desert soil and the lowest in forest soil. Substantially higher contributions of SIC to STC in desert, grassland and agricultural soils, compared to forest soil, would correspond to the significantly lower SOC levels in the former soil types. These results imply that under either high or low SOC conditions, the accumulation of SIC in many soils *via* carbonate mineral formation is limited, which might control the related occurrence of metals, cations, and anions[31,35–38]. This further supports that desert soils act as a major store of SIC and DIC_{LS+CS}, the main fractions of which occur mostly in carbonate mineral forms[7,39,40].

The stable isotopes of soil organic carbon (δ^{13}C-SOC) values appear mostly depleted or highly enriched in forest soils (from −26.93‰ to -21.04‰, average −24.76 ± 2.25‰), which indicates the occurrence of C sequestration upon uptake of CO_2 or DIC deriving from SOC or DOC_{LS+CS} degradation[41]. On average, δ^{13}C-SOC shows to be highly depleted in agricultural soils (-25.47 ± 0.98‰), followed by grassland (-24.85 ± 1.23‰) and forest, but highly enriched in desert soils (-23.39 ± 1.03‰). In all soil types, the δ^{13}C-SOC values appear depleted compared to atmospheric CO_2 (δ^{13}C-DIC, 8.4‰ [42]), suggesting that SOC, specifically lichen-associated cyanobacterial-fungal symbioses[16,17] is not directly related to atmospheric CO_2 uptake. However, the δ^{13}C-SOC values are quite similar in the upper top layers (0–20 cm: -27.3‰ to -19.4‰) and are lower in the deeper profiles (60–120 cm: -27.5‰ to -21.7‰)[23,43]. Such depleted δ^{13}C-SOC values might derive from fresh terrestrial plant materials, whilst enriched values might result from degradative carbon losses[41] with subsequent generations of DIC and/or CO_2 [41,44,45]. These results are further supported by the negative correlation between δ^{13}C-SOC and SOC, which indicates that SOC continuously enriched in δ^{13}C sequentially releases enriched DIC, which is subject to further sequential uptake[41], resulting in a net enrichment of δ^{13}C in SOC.

Similar to SOC, the highest contents of DOC_{LS} and DOC_{CS} occur in forest soils (164 ± 110 and 889 ± 572 mg/kg, respectively), which are significantly higher than, respectively, agricultural (92% and 18.0%, respectively), grassland (109% and 58.6%, respectively) and desert soils (847% and 519%, respectively; Fig. 1). The percentage contributions of soluble DOC_{LS} and DOC_{CS} to SOC followed the order: desert soils (1.5 ± 0.6% and 13.4 ± 10.4%, respectively) > agricultural soils (0.88 ± 0.56% and 5.6 ± 3.0%) > grassland soils (0.76 ± 0.40% and 4.5 ± 3.0%) > forest soils (0.37 ± 0.14% and 2.1 ± 1.0%), respectively. These results suggest that desert DOC_{LS} exhibits the highest lability, indicating the highest mineral instability and degradability in both water- and alkali-extracted dissolved organic matter $(DOM)_{LS+CS}$, which gradually decreases in agricultural, grassland, and forest soils. The lability of soil DOC_{LS} (or the mineral instability) presumably results from mineral-associated SOC, which primarily derives from either plant litter[46–48] or directly from anoxygenic photosynthetic microorganisms[15]. The strong correlation between DOC_{LS} and DOC_{CS} (Fig. 2a) indicates that the former would originate from the latter[33], possibly through heterotrophic respiration at the microbe-mineral interface[49,50].

Similar to DOC_{LS+CS}, DIC_{LS} and DIC_{CS} did not reach the highest amount in the same soil type. In contrast, DIC_{LS} showed the highest level in agricultural soils (144.2 ± 67.4 mg/kg), which is significantly higher than grassland soils (68%), forest soils (86%), and desert soils (120%). Differently, DIC_{CS} showed the highest concentration in forest soils (532 ± 486 mg/kg), which is significantly higher than grassland soils (69.0%), agricultural soils (157%), and desert soils (278%). The high DIC_{LS} and the relatively low DIC_{CS} in agricultural soils would indicate that DIC in its CS form are more susceptible to mineralization in agricultural soils[33], which correspondingly leads to enhanced DIC_{LS}. Furthermore, DIC_{CS} values show a significant positive correlation with DOC_{LS} and DOC_{CS} (Table 2), which would suggest that SOC or DOC_{CS} mineralization[33] *via* heterotrophic respiration[49,50] could give major contribution to DIC and/or CO_2 [41,44,45].

Furthermore, the contribution of DIC_{LS} to SIC followed the order: agricultural soils (1.1 ± 0.5%) > grassland soils (0.92 ± 0.85%) > desert soils (0.86 ± 0.30%) > forest soils (0.76 ± 0.64%), while the DIC_{CS} contribution order was grassland soils (3.6 ± 5.1%) > forest soils (2.0 ± 0.9% > desert soils (2.0 ± 0.5%) > agricultural soils (1.6 ± 0.8%). These results suggest that different land uses produce distinct DIC_{LS+CS} characteristics. The fact that DIC_{LS} was much higher (~ 280%) than DOC_{LS} in desert soils would possibly derive from the high presence of sand (45 ± 27%) rich in carbonate and silicate minerals[23,51]. Furthermore, sand appears to induce significant CO_2 uptake via photosynthetic microorganisms, with consequent neoformation of SOC-associated minerals[39,40,52,53]. The significant negative correlation between DIC_{LS} and δ^{13}C-SOC, and the insignificant correlation between DIC_{CS} and δ^{13}C-SOC (Table 2) strongly suggests that SOC primarily arises from inorganic carbon fixation (mostly DIC_{LS}) in drying-affected soil types. Similarly, such mineral neoformation[54,55] is further confirmed by the significant negative correlation between δ^{13}C-SOC and $SiO_3^{2-}{}_{CS}$ (Table 2).

The strong correlation ($p < 0.001$) of DOC_{CS} with both DIC_{CS} and DIC_{LS}, and the positive correlation of SOC with DIC_{CS} (but not with DIC_{LS}, Table S2) would suggest that DIC_{CS} mostly derives from SOC and/or DOC_{CS} mineralization[23,33]. Furthermore, the strong correlation of SiO_3^{2-} with both DIC_{LS} and DIC_{CS} would strongly

Soil type	ID	Soil Classfication[a]	pH	Water EC mS/cm	content (%)	STC g/kg	STN g/kg	STH g/kg	STS g/kg	SOC g/kg	δ^{13}C-SOC (‰)	SIC g/kg	C/*N*	Soil texture[a] Sand %	Silt %	Clay %
Forest	XJ-S-1	Greyzem	5.63	0.518	17.9	-	2.73	11.0	0.281	46.5	-25.06	-	-	6.2	85.5	8.3
	XJ-S-3	Greyzem	7.56	3.6	0.9	15.8	6.62	5.93	4.12	5.86	-21.04	9.9	2.98	32.4	62.1	5.5
	XJ-S-4	Greyzem	6.72	0.144	36.7	135.7	7.96	21.6	1.05	107.1	-24.76	28.5	21.3	13.6	75.7	10.8
	XJ-S-5	Greyzem	6.85	0.252	13.3	101.4	6.86	19.3	0.766	79.7	-26.02	21.7	18.5	14.2	77.4	8.3
	XJ-S-13	Leptosols	7.41	0.198	8.9	26.2	2.05	8.23	0.497	18.9	-26.93	7.3	16.0	62.7	29.1	8.2
Average (forest)	5		6.83 ± 0.76	0.94 ± 1.5	15.6 ± 13.4	69.8 ± 58.2	5.2 ± 2.7	13.2 ± 6.9	1.3 ± 1.6	51.6 ± 42.0	24.76 ± 2.25	16.9 ± 10.0	15.7 ± 7.4	25.8 ± 22.8	66.0 ± 22.3	8.2 ± 1.9
Agriculture	XJ-S-14	Kastanozems	7.48	0.283	6.3	32.5	2.19	7.1	0.465	19.5	-26.16	13.1	18.5	12.1	81.1	6.8
	XJ-S-15	Anthrosols	7.81	0.284	1.0	20.7	1.34	6.4	0.265	10.5	-25.74	10.2	19.3	9.5	82.6	8.0
	XJ-S-16	Gypsosols	7.21	0.634	13.9	41.5	3.06	9.6	0.639	24.3	-25.97	17.2	16.9	54.4	32.6	13.0
	XJ-S-17	Gypsosols	7.96	10.2	1.2	13.3	0.395	6.0	5.0	0.743	-24.02	12.6	42.2	48.6	46.7	4.7
Average (agriculture)	4		7.62 ± 0.34	2.84 ± 4.9	5.6 ± 6.1	27.0 ± 12.5	1.8 ± 1.1	7.3 ± 1.6	1.6 ± 2.3	13.8 ± 10.4	25.47 ± 0.98	13.3 ± 2.90	24.3 ± 12.0	31.1 ± 23.6	60.7 ± 25.1	8.1 ± 3.5
Grassland	XJ-S-2	Calcisol	7.15	2.47	2.9	16.9	2.32	5.90	4.21	5.284	-22.82	11.6	9.1	12.6	81.1	6.3
	XJ-S-9	Arenosols	6.97	0.252	25.9	75.2	7.59	16.4	8.1	53.8	-25.98	21.4	12.4	12.1	78.3	9.6
	XJ-S-12	Kastanozems	7.96	0.302	2.39	29.9	2.75	6.88	0.792	23.3	-26.22	6.6	13.6	49.0	41.8	9.2
	XJ-S-21	Solonchaks	7.68	6.13	0.375	13.0	0.469	3.63	0.800	1.449	-24.33	11.5	34.5	57.6	39.8	2.6
	XJ-S-22	Solonchaks	7.49	0.129	5.63	18.6	0.912	5.81	0.291	8.623	-24.89	10.0	25.5	53.7	39.7	6.6
	XJ-S-23	Gypsosols	7.99	11.4	2.18	11.5	0.605	9.56	23.8	1.290	-24.87	10.2	23.7	56.3	41.3	2.4
Average (grassland)	6		7.54 ± 0.42	3.44 ± 4.5	6.6 ± 9.6	27.5 ± 24.3	2.4 ± 2.7	8.0 ± 4.5	6.3 ± 9.1	15.6 ± 20.4	24.85 ± 1.23	11.9 ± 5.02	19.8 ± 9.7	40.2 ± 21.8	53.7 ± 20.2	6.1 ± 3.1
Desert land	XJ-S-7	Anthrosols	7.61	8.2	-	8.0	0.554	10.7	24.6	0.873	-22.77	7.17	18.2	22.3	70.4	7.3
	XJ-S-8	Anthrosols	7.54	2.33	1.64	5.5	0.228	6.36	9.09	1.61	-21.99	3.92	30.3	68.4	27.6	5.0
	XJ-S-10	Gypsosols	7.71	4.04	1.04	8.5	0.208	6.75	5.55	1.39	-24.43	7.13	51.2	12.1	78.3	9.6
	XJ-S-11	Gypsosols	7.81	2.48	0.550	8.2	0.197	3.51	2.14	0.842	-23.42	7.34	51.8	48.5	43.3	7.9
	XJ-S-18	Gypsosols	8.04	8.01	3.41	15.7	0.363	3.98	2.28	1.34	-24.31	14.4	54.1	73.0	17.9	9.1
Average (desert land)	5	-	7.74 ± 0.20	5.0 ± 2.9	1.7 ± 1.5	9.2 ± 3.8	0.31 ± 0.15	6.3 ± 2.8	8.7 ± 9.3	1.21 ± 0.340	23.39 ± 1.03	7.99 ± 3.85	41.1 ± 16.0	44.9 ± 27.1	47.5 ± 26.3	7.8 ± 1.8
Range among all soils	—	—	5.63–8.04	0.13–11.4	0.38-49.0	5.5-135.7	0.20-8.0	3.5–19.3	0.26–24.6	0.743–107.1	-26.93–21.04	3.92–28.5	2.4–43.3	6.2–73.0	17.9–85.5	2.4–13.0

Table 1. Biogeochemical properties of the four dryland soil types, i.e., forest, agriculture, grassland and desert soils, examined in this work. Soil classification is based on the Harmonized World Soil Database (HWSD). The sign '±' indicates the standard deviation (STDEV) among soil samples.

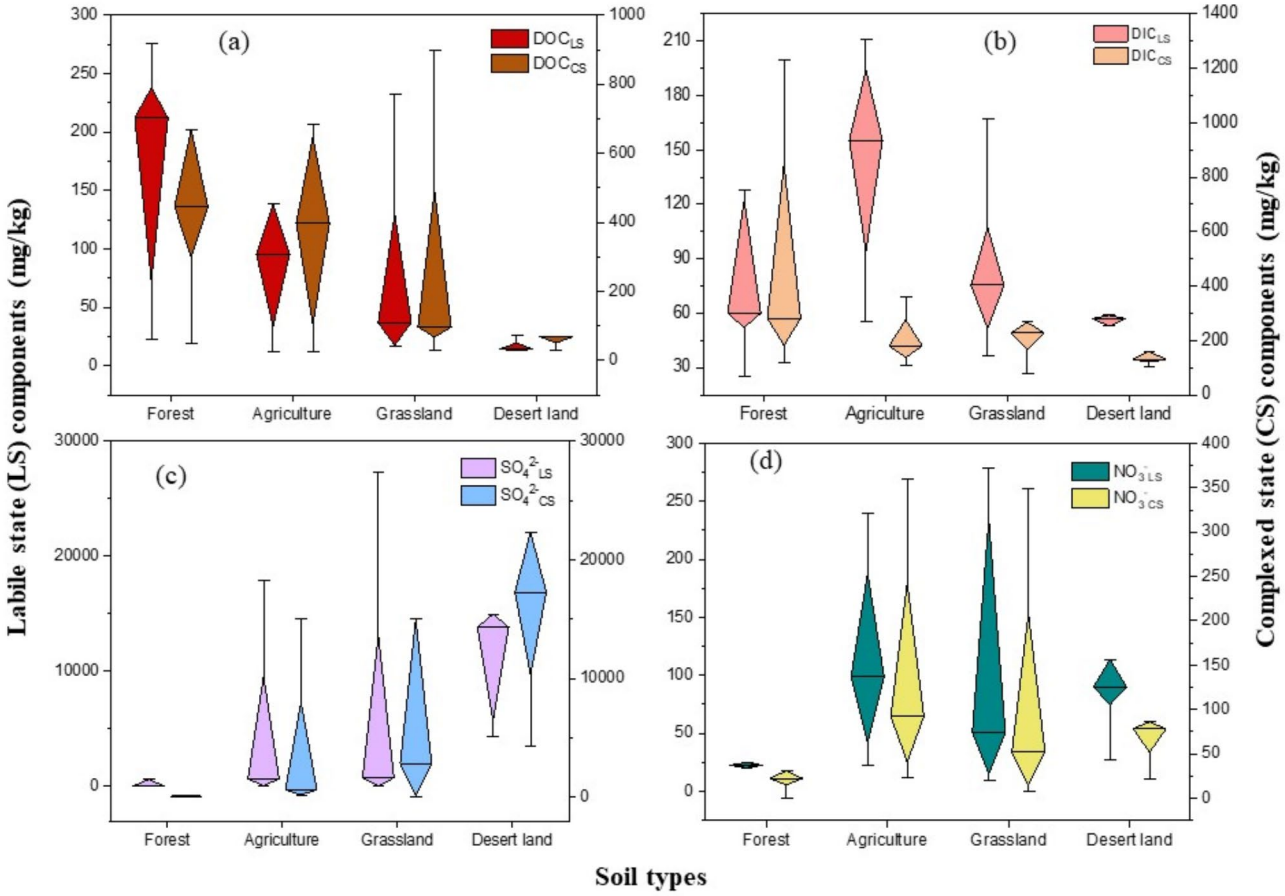

Fig. 1. Concentrations of labile state (LS) and complexed state (CS) dissolved organic carbon (DOC_{LS} and DOC_{CS}, **a**), dissolved inorganic carbon (DIC_{LS} and DIC_{CS}, **b**), sulfate ($SO_4^{2-}{}_{LS}$ and $SO_4^{2-}{}_{CS}$, **c**), nitrate ($NO_3^-{}_{LS}$ and $NO_3^-{}_{CS}$, **d**) in forest, agriculture, grassland and desert dry-affected soils.

support the at least partial origin of both DIC forms from silicate minerals, mostly clay, LDHs-like and Fe minerals-associated carbonates[31,35,38]. Therefore, DIC_{LS+CS} dynamics would predominantly involve, on the one side, the production resulting from dissolution and mineralization of SOC-bound clay, carbonate or LDHs-like minerals. On the other side, it would include the generation from simultaneous SOC mineralization[31,35,36,56], which also leads to the export of DOM_{LS+CS}, thereby influencing DOM dynamics in diverse soil types.

Biogeochemical cycling of STS and $SO_4^{2-}{}_{LS+CS}$

Soil total sulfur (STS) showed, on average, the highest levels in desert soils (8.7 ± 9.3 g/kg), which were 38.0% higher than those found in grassland soils, 444% higher than in agricultural soils, and 570% higher tahn in forest soils (Table 1). Similarly, the $SO_4^{2-}{}_{LS}$ and $SO_4^{2-}{}_{CS}$ fractions show significant variation among soil types (34-3.2×10^4 mg/kg and 53-5.6×10^4 mg/kg, respectively), with highest values on average in desert soils ($1.4 \pm 1.1 \times 10^4$ and ($1.9 \pm 1.4 \times 10^4$ mg/kg, respectively) that are respectively 103% and 47% higher than those in grassland soils, 196% and 360% higher compared to agricultural soils, and 481% and 409% higher compared to forest soils (Fig. 1c). In particular, all desert soils, one forest soil, one agricultural soil, and three grassland soils feature extremely high STS and $SO_4^{2-}{}_{LS+CS}$ values, which are key signatures of saline-alkali soils[24–27].

The very high $SO_4^{2-}{}_{LS+CS}$ and STS values in desert and grassland soils might arise from similar phenomena, i.e., the sulfide-dependent anoxygenic photosynthetic sequestration of S and C by COS uptake[14–18]. These processes would subsequently result in the high production and sequestration of $SO_4^{2-}{}_{LS+CS}$ *via* redox reactions, leading to the generation of $S^0 \leftrightarrow SO_4^{2-} \leftrightarrow S^{2-}/S_2^{2-} \leftrightarrow SO_4^{2-}$ (Fig. 1c)[28–30,57,58]. Significant positive correlations between $SO_4^{2-}{}_{LS+CS}$ and δ^{13}C-SOC values (Table 2; Fig. 3) suggest that sulfur sequestration occurs through SO_4^{2-}-mediated redox processes.

The occurrence of high SO_4^{2-} contents might be ascribed to several factors, such as no uptake by plants, no leaching by rainwater due to plain land, high rates of evapotranspiration, and rapid elemental conversion of S to SO_4^{2-} in the presence of abundant O_2 in alkaline soils[58,59]. In essence, high $SO_4^{2-}{}_{LS+CS}$ values might have substantial impact on the SOC-associated organo-mineral complexes and on C stabilization in drying-affected soils through SOC and/or DOM_{LS+CS} mineralization, *via* microbial $SO_4^{2-}{}_{LS+CS}$ reduction[28–30]. This might be the key reason for extended SOC and/or DOM mineralization under drying-wetting cycles in these soil types[60–62].

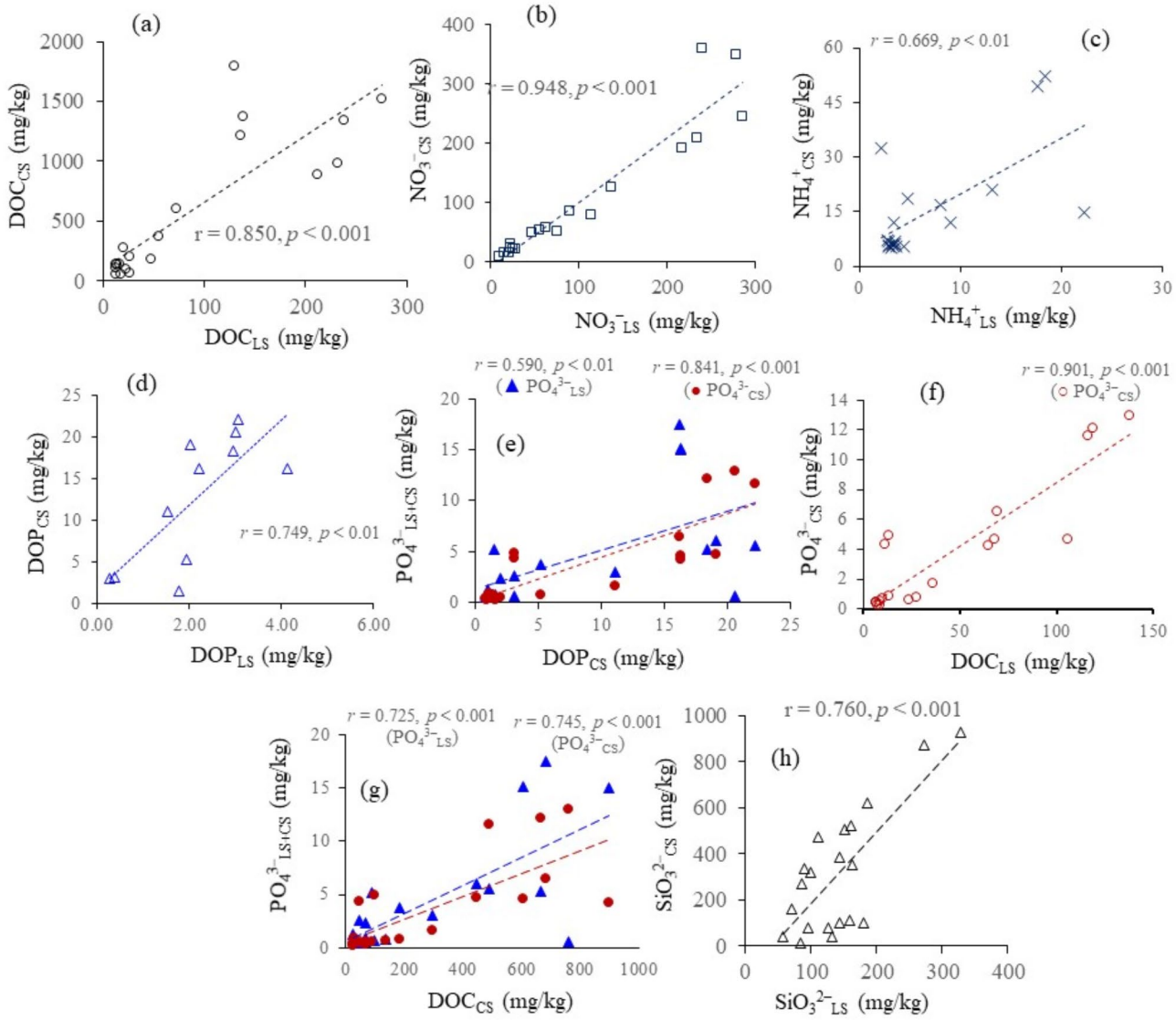

Fig. 2. Linear Pearson correlations between some relevant parameters of dry-affected soils studied: (**a**) DOC_{LS} vs. DOC_{CS}, (**b**) $NO_3^-{}_{LS}$ vs. $NO_3^-{}_{CS}$, (**c**) $NH_4^+{}_{LS}$ vs. $NH_4^+{}_{CS}$, (**d**) DOP_{LS} vs. DOP_{CS}, (**e**) DOP_{CS} vs. $PO_4^{3-}{}_{LS+CS}$, (**f**) DOC_{LS} vs. $PO_4^{3-}{}_{CS}$, (**g**) DOC_{CS} vs. $PO_4^{3-}{}_{LS+CS}$, and (**h**) $SiO_3^{2-}{}_{LS}$ vs. $SiO_3^{2-}{}_{CS}$. The significance of the *p*-values are presented at the level $p < 0.01$ and $p < 0.001$.

Biogeochemical cycling of STN and N-containing components

Similar to SOC, STN showed the highest content in forest soils (5.2 ± 2.7 g/kg), which was 117% higher compared to grassland soils, 190% higher compared to agricultural soils, and even 1600% higher compared to desert soils (Table 1). Correspondingly, the lowest C/N ratio was measured in forest soils (average: 15.7 ± 7.4), followed by grassland soils (19.8 ± 9.7), agricultural soils (24.3 ± 12.0), and desert soils (41.1 ± 16.0). The $NO_3^-{}_{LS}$ and $NO_3^-{}_{CS}$ concentrations varied widely (2.3-284.8 and 7.7-359.1 mg/kg, respectively) among the examined soils showing, on average, the lowest level in forest soils (57 ± 89 and 84 ± 39 mg/kg, respectively). Furthermore, the highest levels of $NO_3^-{}_{LS}$ occurred in desert soils (118 ± 98), followed by agricultural and grassland soils (115 ± 95 and 114 ± 136 mg/kg, respectively), while the highest $NO_3^-{}_{CS}$ occurred in agricultural soils (142 ± 151 mg/kg), followed by grassland and desert soils (106 ± 118 and 97 ± 87 mg/kg, respectively (Fig. 1d). The high variation of $NO_3^-{}_{LS+CS}$ contents in the different soil types might arise from drying-rewetting N-mineralization processes, whereas NO_3^- can remain stable and steady for more than a month after the last stress by rewetting-drying[63]. Similarly, drying-wetting cycles may cause a decrease of mineral N and an increase or decrease of NO_3^-, depending on soil types, C compounds, and drying intensity[63–65], which are possibly related to a decline of soil fungi under dry conditions[63,64]. In particular, the low levels of $NO_3^-{}_{LS+CS}$ in forest soils might arise from high N mineralization and gaseous losses of N via nitrification followed by denitrification[62–64], possibly caused by the availability of water inside soils covered by dense forest.

A significant positive correlation between $NO_3^-{}_{LS}$ and $NO_3^-{}_{CS}$, and between each of them and STS and $SO_4^{2-}{}_{LS+CS}$ (Fig. 1b; Table 2), would suggest that $NO_3^-{}_{LS}$ and $NO_3^-{}_{CS}$ originate from similar sources by a two-

Parameters	pH	EC	Water Contents	STN	STH	STS	SOC	δ^{13}C-SOC	SIC
pH	1.000								
EC	**0.518***	1.000							
Water Contents	**−0.704****	**−0.449***	1.000						
STN	**−0.532***	**−0.484***	**0.748****	1.000					
STH	**−0.597***	-0.312	**0.877****	**0.780****	1.000				
STS	0.255	**0.659***	-0.153	-0.221	0.078	1.000			
SOC	**−0.676****	**−0.519***	**0.904****	**0.819****	**0.918****	-0.285	1.000		
δ^{13}C -SOC	0.168	0.406	-0.359	-0.156	-0.327	0.347	-0.406	1.000	
SIC	**−0.713****	-0.242	**0.867****	**0.756****	**0.793****	-0.241	**0.858****	-0.331	1.000
Sand (%)	**0.545***	0.367	-0.418	**−0.477***	**−0.495***	0.054	**−0.474***	0.101	-0.396
Silt (%)	**−0.521***	-0.312	0.365	**0.4434***	**0.461***	-0.010	0.429	-0.051	0.353
Clay (%)	-0.342	**−0.570***	**0.555***	0.391	0.410	-0.382	**0.496***	-0.425	0.424
$SO_4^{2-}{}_{LS}$	0.362	**0.784****	**−0.451***	-0.393	-0.164	**0.888****	**−0.482***	**0.587***	-0.401
$SO_4^{2-}{}_{CS}$	0.364	**0.784****	-0.372	-0.352	-0.117	**0.926****	-0.434	**0.490***	-0.352
DOC_{LS}	**−0.804****	**−0.597***	**0.850****	**0.717****	**0.776****	-0.326	**0.878****	**−0.544***	**0.804****
DOC_{CS}	**−0.554***	**−0.620***	**0.610***	**0.508***	**0.518***	-0.360	**0.663****	**−0.606***	**0.456***
DIC_{LS}	0.213	-0.420	-0.122	0.006	-0.132	**−0.506***	0.024	**−0.587***	0.059
DIC_{CS}	**−0.640***	-0.424	**0.527***	0.330	0.371	-0.346	**0.578***	-0.316	0.394
$SiO_3^{2-}{}_{LS}$	-0.115	-0.383	-0.063	-0.064	-0.172	-0.261	-0.132	-0.295	-0.115
$SiO_3^{2-}{}_{CS}$	-0.241	**−0.529***	0.189	0.105	0.013	**−0.535***	0.179	**−0.697****	0.162
$NO_3^{-}{}_{LS}$	**0.462***	**0.828****	-0.379	-0.265	-0.219	**0.641***	**−0.447***	0.368	-0.199
$NO_3^{-}{}_{CS}$	**0.478***	**0.864****	-0.308	-0.278	-0.178	**0.599***	-0.388	0.261	-0.151
$NH_4^{+}{}_{LS}$	-0.306	-0.437	**0.714****	**0.774****	**0.804****	-0.129	**0.802****	**−0.505***	**0.697****
$NH_4^{+}{}_{CS}$	**−0.666****	**−0.502***	**0.738****	**0.703****	**0.832****	-0.337	**0.940****	-0.420	**0.756****
$NO_2^{-}{}_{LS}$	-0.177	**−0.502***	0.248	0.299	0.227	-0.358	0.293	**−0.714****	0.304
$NO_2^{-}{}_{CS}$	**−0.844****	**−0.475***	**0.832****	**0.617***	**0.707****	-0.229	**0.795****	**−0.455***	**0.804****
$PO_4^{3-}{}_{LS}$	-0.012	**−0.489***	0.194	0.276	0.150	-0.358	0.263	**−0.562***	0.243
$PO_4^{3-}{}_{CS}$	**−0.823****	**−0.515***	**0.845****	**0.751****	**0.674****	-0.257	**0.779****	-0.259	**0.783****
DOP_{LS}	-0.297	**−0.721****	0.510	0.083	0.398	-0.194	0.458	**−0.645***	0.427
DOP_{CS}	**−0.683****	**−0.642***	**0.771****	**0.713****	**0.708****	-0.350	**0.807****	**−0.639***	**0.671***

Parameters	Sand (%)	Silt (%)	Clay (%)	$SO_4^{2-}{}_{LS}$	$SO_4^{2-}{}_{CS}$	DOC_{LS}	DOC_{CS}	DIC_{LS}	DIC_{CS}
pH									
EC									
Water Contents									
STN									
STH									
STS									
SOC									
δ^{13}C -SOC									
SIC									
Sand (%)	1.000								
Silt (%)	**−0.994****	1.000							
Clay (%)	-0.271	0.160	1.000						
$SO_4^{2-}{}_{LS}$	0.092	-0.038	**−0.481***	1.000					
$SO_4^{2-}{}_{CS}$	0.178	-0.120	**−0.533***	**0.944****	1.000				
DOC_{LS}	**−0.517***	**0.467***	**0.543***	**−0.566***	**−0.519***	1.000			
DOC_{CS}	-0.367	0.310	0.574*	**−0.552***	**−0.521***	**0.850****	1.000		
DIC_{LS}	0.119	-0.163	0.338	**−0.541***	**−0.511***	0.131	0.436	1.000	
DIC_{CS}	-0.317	0.285	0.348	-0.436	-0.412	**0.733****	**0.789****	0.022	1.000

Continued

Parameters	Sand (%)	Silt (%)	Clay (%)	$SO_4^{2-}_{LS}$	$SO_4^{2-}_{CS}$	DOC_{LS}	DOC_{CS}	DIC_{LS}	DIC_{CS}
$SiO_3^{2-}_{LS}$	-0.061	0.025	0.336	-0.222	-0.251	0.098	0.384	**0.652***	0.008
$SiO_3^{2-}_{CS}$	0.008	-0.056	0.404	**−0.659***	**−0.609***	0.442	**0.648***	**0.795****	0.295
$NO_3^-_{LS}$	0.254	-0.207	**−0.483***	**−0.443***	**0.696****	**−0.494***	**−0.443***	-0.282	-0.436
$NO_3^-_{CS}$	0.250	-0.194	**−0.535***	**0.676***	**0.675***	-0.415	-0.379	-0.362	-0.369
$NH_4^+_{LS}$	-0.330	0.290	0.415	-0.406	-0.366	**0.704****	**0.576***	0.158	0.296
$NH_4^+_{CS}$	**−0.458***	0.417	**0.455***	**−0.469***	-0.425	**0.842****	**0.695****	0.141	**0.630***
$NO_2^-_{LS}$	-0.111	0.061	**0.446***	**−0.557***	**−0.484***	**0.499***	**0.660***	**0.761****	0.158
$NO_2^-_{CS}$	**−0.496***	**0.456***	**0.458***	**−0.455***	-0.402	**0.953****	**0.780****	-0.083	**0.787****
$PO_4^{3-}_{LS}$	-0.079	0.031	0.424	**−0.482***	**−0.450***	0.413	**0.725****	**0.837****	0.268
$PO_4^{3-}_{CS}$	**−0.589***	**0.553***	**0.444***	-0.433	-0.413	**0.901****	**0.745****	-0.073	**0.713****
DOP_{LS}	-0.337	0.300	0.530	**−0.725***	**−0.750***	**0.717***	**0.755***	0.290	0.478
DOP_{CS}	**−0.446***	0.391	**0.574***	**−0.601***	**−0.551***	**0.956****	**0.912****	0.321	**0.649***

Parameters	$SiO_3^{2-}_{LS}$	$SiO_3^{2-}_{CS}$	$NO_3^-_{LS}$	$NO_3^-_{CS}$	$NH_4^+_{LS}$	$NH_4^+_{CS}$	$NO_2^-_{LS}$	$NO_2^-_{CS}$	$PO_4^{3-}_{LS}$	$PO_4^{3-}_{CS}$	DOP_{LS}	DOP_{CS}
pH												
EC												
Water Contents												
STN												
STH												
STS												
SOC												
$\delta^{13}C$ -SOC												
SIC												
Sand (%)												
Silt (%)												
Clay (%)												
$SO_4^{2-}_{LS}$												
$SO_4^{2-}_{CS}$												
DOC_{LS}												
DOC_{CS}												
DIC_{LS}												
DIC_{CS}												
$SiO_3^{2-}_{LS}$	1.000											
$SiO_3^{2-}_{CS}$	**0.760****	1.000										
$NO_3^-_{LS}$	-0.131	-0.300	1.000									
$NO_3^-_{CS}$	-0.169	-0.283	**0.948****	1.000								
$NH_4^+_{LS}$	-0.175	0.166	-0.332	-0.347	1.000							
$NH_4^+_{CS}$	-0.045	0.243	-0.439	-0.367	**0.669****	1.000						
$NO_2^-_{LS}$	**0.673****	**0.872****	-0.197	-0.195	0.380	0.343	1.000					
$NO_2^-_{CS}$	0.006	0.335	-0.414	-0.307	**0.563***	**0.740****	0.354	1.000				
$PO_4^{3-}_{LS}$	**0.672****	**0.780***	-0.205	-0.248	0.384	0.314	**0.840****	0.224	1.000			
$PO_4^{3-}_{CS}$	0.074	0.284	-0.417	-0.349	**0.579***	**0.672****	0.295	**0.914****	0.282	1.000		
DOP_{LS}	0.103	**0.657***	-0.316	-0.260	0.423	0.410	**0.632***	**0.627***	0.576	0.535	1.000	
DOP_{CS}	0.262	**0.592***	**−0.467***	-0.392	**0.746****	**0.777****	**0.674****	**0.876****	**0.590***	**0.841****	**0.749***	1.000

Table 2. Pearson correlations between the parameters measured in 20 soil samples under four land-use types, i.e., forest, agriculture, grassland and desert, collected from the Xinjiang Uyghur autonomous region, China. Statistical significance is reported as either $0.05 > p > 0.01^{*}$ or $p < 0.01^{**}$)

step pathway: there is NH_4^+ production[25,66] from SOC or DOM respiration and mineralization *via* microbial $SO_4^{2-}_{LS+CS}$ reduction[28–30], followed by autotrophic NH_4^+ oxidation into NO_3^- by chemolithoautotrophs[67,68]. The $NH_4^+_{LS}$ and $NH_4^+_{CS}$ contents vary largely among soil types (2.2–22.2 and 5.1–52.3 mg/kg, respectively), being highest on average in forest soils (10.0 ± 7.8 and 30.7 ± 20.8 mg/kg, respectively) and lowest in desert soils (3.3 ± 0.6 and 5.6 ± 0.4 mg/kg, respectively; Fig. 4b). The high level of $NH_4^+_{LS+CS}$ in forest soils might be due to the dissolution and mineralization of NH_4^+-bound minerals and N-bound SOC and/or DOM[31,38,69,70], which

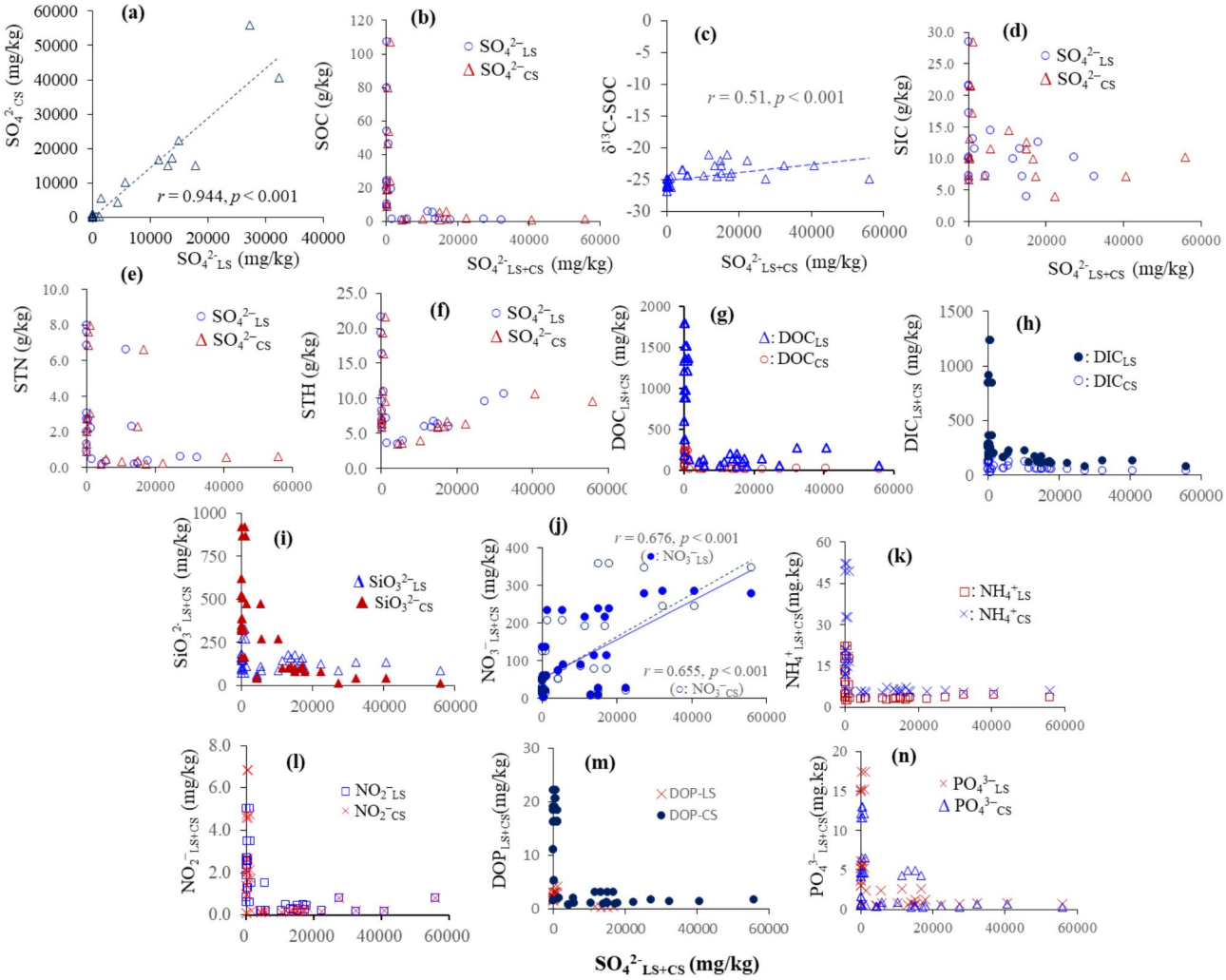

Fig. 3. Pearson correlations between $SO_4^{2-}{}_{LS}$ and $SO_4^{2-}{}_{CS}$ (**a**), $SO_4^{2-}{}_{LS+CS}$ and the stable isotopes of δ^{13}C-SOC (**c**), and $SO_4^{2-}{}_{LS+CS}$ and $NO_3^{-}{}_{LS+CS}$ (**j**) in drying-affected soils studied, where the significance of the *p*-values for $SO_4^{2-}{}_{LS+CS}$ vs. $NO_3^{-}{}_{LS+CS}$ are at the level $p < 0.001$. The relationships between $SO_4^{2-}{}_{LS+CS}$ and soil relevant components in drying-affected soils studied showed that low levels of STS are associated with high levels of these components, and conversely, high levels of STS correspond to low levels of the relevant soil components. The relationships include $SO_4^{2-}{}_{LS+CS}$ with SOC (**b**), SIC (**d**), STN (**e**), STH (**f**), DOC_{LS+CS} (**g**), DIC_{LS+CS} (**h**), $SiO_3^{2-}{}_{LS+CS}$ (**i**), $NH_4^{+}{}_{LS+CS}$ (**k**), $NO_2^{-}{}_{LS+CS}$ (**l**), DOP_{LS+CS} (**m**), and $PO_4^{3-}{}_{LS+CS}$ (**n**).

remains stable due to the relatively low presence of SO_4^{2-} in forest soils (Fig. 1c). Furthermore, clay contents show a significant positive correlation with $NH_4^{+}{}_{CS}$ (Table 2), which suggests that clay minerals might be a source of NH_4^{+}[71]. The strong positive correlation between $NH_4^{+}{}_{LS}$ and $NH_4^{+}{}_{CS}$ (Fig. 2c) suggests that both would likely originate from similar sources. Interestingly, the low $NH_4^{+}{}_{LS+CS}$ in desert soils might be related to the abundance of SO_4^{2-} and $NO_3^{-}{}_{LS+CS}$ (Fig. 1d). These results are further supported by the significant negative correlation of $SO_4^{2-}{}_{LS}$ with $NH_4^{+}{}_{CS}$ and by the significant positive correlation between $SO_4^{2-}{}_{CS}$ and $NO_3^{-}{}_{LS+CS}$ (Table 2). Therefore, SO_4^{2-} plays pivotal roles in the steady-state occurrence and levels of $NO_3^{-}{}_{LS+CS}$ and $NH_4^{+}{}_{LS+CS}$. The $NO_2^{-}{}_{LS}$ and $NO_2^{-}{}_{CS}$ concentrations appeared relatively low in all soil types (0.2-5.0 and 0.1–6.8 mg/kg, respectively) and were, on average, the lowest in desert soils (0.21 ± 0.03 and 0.17 ± 0.03 mg/kg, respectively), and the highest in agricultural soils ($NO_2^{-}{}_{LS}$, 2.8 ± 1.9 mg/kg) and forest soils ($NO_2^{-}{}_{CS}$, 3.2 ± 2.6 mg/kg) (Fig. 4a). The remaining text of this subsection is discussed in the SI.

Biogeochemical cycling of dissolved organic phosphorus and $PO_4^{3-}{}_{LS+CS}$

The $PO_4^{3-}{}_{LS}$ and $PO_4^{3-}{}_{CS}$ concentrations showed wide variation (0.5–17.5 and 0.3–13.0 mg/kg, respectively), with the highest average $PO_4^{3-}{}_{LS}$ level in agricultural soils (9.4 ± 8.1 mg/kg), which is 91% higher compared to grassland soils, 168% higher compared to forest soils, and 1220% higher compared to desert soils (Fig. 4c). Differently, $PO_4^{3-}{}_{CS}$ was the highest (7.2 ± 5.1 mg/kg) in forest soils, that is 94% higher compared to grassland soils, 130% higher compared to agricultural soils, and 1200% higher compared to desert soils. The dissolved organic phosphorus $(DOP)_{LS}$ value (0.3–18.1 mg/kg) was a bit lower than DOP_{CS} (0.8–22.2 mg/kg), with DOP_{LS}

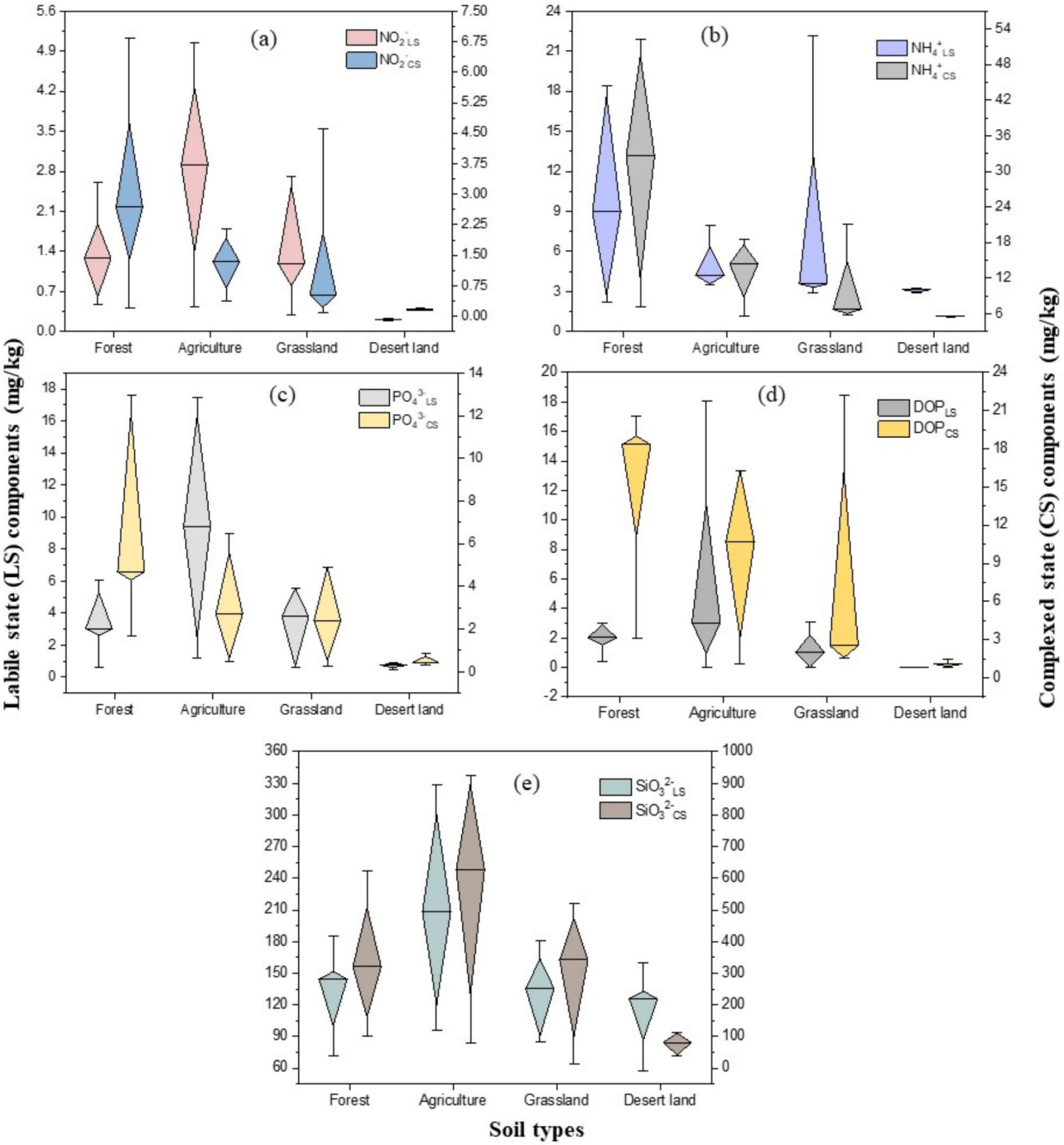

Fig. 4. Concentrations of labile state (LS) and complexed state (CS) nitrite ($NO_2^-{}_{LS}$ and $NO_2^-{}_{CS}$, **a**), ammonium ($NH_4^+{}_{LS}$ and $NH_4^+{}_{CS}$, **b**), phosphate ($PO_4^{3-}{}_{LS}$ and $PO_4^{3-}{}_{CS}$, **c**), dissolved organic phosphorus (DOP_{LS} and DOP_{CS}, **d**) and silicate ion ($SiO_3^{2-}{}_{LS}$ and $SiO_3^{2-}{}_{CS}$, **e**) in forest, agriculture, grassland and desert dry-affected soils.

showing the highest value (8.1 ± 8.7 mg/kg) in agricultural soils, namely 310% higher than in forest soils and 340% higher than in grassland soils, while DOP_{LS} was undetectable in desert soils (Fig. 4d). Differently, DOP_{CS} was highest (14.4 ± 7.3 mg/kg) in forest soils, which is 49% higher than in agricultural soils, 86% higher than in grassland soils, and 1250% higher than in desert soils. In particular, high $PO_4^{3-}{}_{LS}$ in agricultural soil might arise from manure application, whereas high $PO_4^{3-}{}_{CS}$ in forest soil might arise from two possible sources via redox cycling[57]: (i) dissolution and mineralization of phosphate minerals[35,57,72–74], and (ii) mineralization of DOP–bound SOC- or DOC-associated minerals[57,73–75]. The latter process is further supported by the significant correlations of DOP_{CS} with $PO_4^{3-}{}_{LS}$ and $PO_4^{3-}{}_{CS}$ (Fig. 2e), and of DOC_{LS} (as well as DOC_{CS}) with $PO_4^{3-}{}_{LS}$ and $PO_4^{3-}{}_{CS}$ (Fig. 2f-g; Table 2). Remarkably, low STS and $SO_4^{2-}{}_{LS+CS}$ contents were well correlated with high

amounts of DOP_{LS+CS}, and $PO_4^{3-}{}_{LS+CS}$, and vice versa (Figs. 3m, n and 5j, k). These results would suggest that STS might be involved in DOP mineralization[57,73–75] through $SO_4^{2-}{}_{LS+CS}$-mediated reduction processes[28,31], whereas the produced PO_4^{3-} might be associated to the neoformation of clay and secondary minerals[31,35,38].

Biogeochemical cycling of $SiO_3^{2-}{}_{LS+CS}$

The $SiO_3^{2-}{}_{LS}$ and $SiO_3^{2-}{}_{CS}$ contents differed substantially among the studied soils ranging, respectively, between 57 and 328 mg/kg and between 13 and 924 mg/kg, with the highest average values in agricultural soils (210 ± 109 and 565 ± 404 mg/kg, respectively). These values were higher by, respectively, 61% and 65% compared to forest soils, 60% and 89% compared to grassland soils, and 87% and 416% compared to desert soils (Fig. 4e). The remaining text of this subsection is discussed in the SI.

Transformation features of humic substances (HS) components

The EEM-PARAFAC model could identify one to three fluorescent components in the water-extracted and alkali-extracted DOM_{CS} or HS_{CS} of the four studied soil types (Fig. 6; Table S2). The three components can be denoted as humic acids (HA), fulvic acids (FA) and protein-like substances (PLS), which collectively define the HS composition[76,77]. Forest soils are characterized by only one component denoted as degraded HA_{LS} with two peaks in a relatively short wavelength region (Table S2). This implies that the other two components, i.e., FA_{LS} and PLS_{LS} of HS_{LS} are completely degraded or mineralized (Fig. 6), thereby suggesting the highly labile and degradative nature of forest HS_{LS} components. Differently, three components (HA_{CS}, FA_{CS} and PLS_{CS}) of HS_{CS} are present in forest soils, with two long-wavelength peaks for HA_{CS} and $FA_{CS,}$ and two protein-like adjacent peaks (260/299, 340 nm) (Fig. 6). These results suggest that HS_{CS} components remain mostly unaffected, i.e., their recalcitrant nature in forest soil, presumably their involvement in organo-minerals complexes[37,78,79].

Agricultural soils featured two components, i.e., degraded HA_{LS} with two peaks and PLS_{LS} with two longer-wavelength peaks (M and T; Table S2 and Fig. 6). These results suggest that HS_{LS} or DOM in agricultural soils may have been degraded due to drying effects. By contrast, HA_{CS} and FA_{CS} in agricultural soils show the peaks (C, M, and A) in relatively long-wavelength regions, implying that these two components remain primarily unaffected as in the case of forest soils. This finding might suggest that HA- and FA-bound organo-minerals in CS forms remain unaffected under extreme drying conditions, as reported in earlier studies[31,79,80]. Differently, the PLS_{CS} showed the complete disappearance of the four peaks of humic-like and protein-like fractions, which subsequently lead to the production of tryptophan-like substances with two new peaks (T, 275/351 nm and

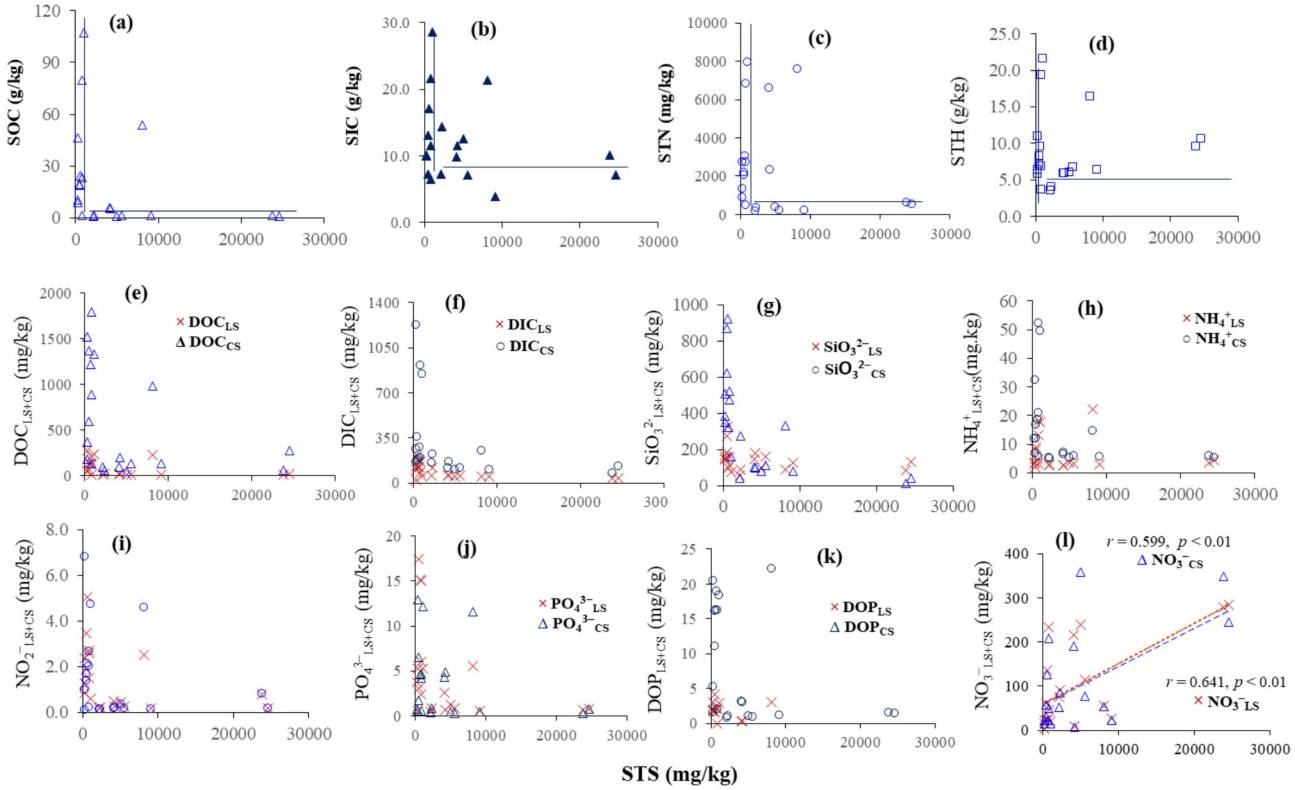

Fig. 5. Relationships between soil total sulfur (STS) and soil relevant components in drying-affected soils studied, showing that low levels of STS are associated with high levels of these components, and conversely, high levels of STS correspond to low levels of the relevant soil components. The relationships shown include STS with SOC (**a**), SIC (**b**), STN (**c**), STH (**d**), DOC_{LS+CS} (**e**), DIC_{LS+CS} (**f**), $SiO_3^{2-}{}_{LS+CS}$ (**g**), $NH_4^+{}_{LS+CS}$ (**h**), $NO_2^-{}_{LS+CS}$ (**i**), $PO_4^{3-}{}_{LS+CS}$ (**j**), and DOP_{LS+CS} (**k**). Pearson correlation of STS with $NO_3^-{}_{LS+CS}$ (**l**) in drying-affected soils studied. The significance of the *p*-values are at the level $p < 0.01$ or $p < 0.001$.

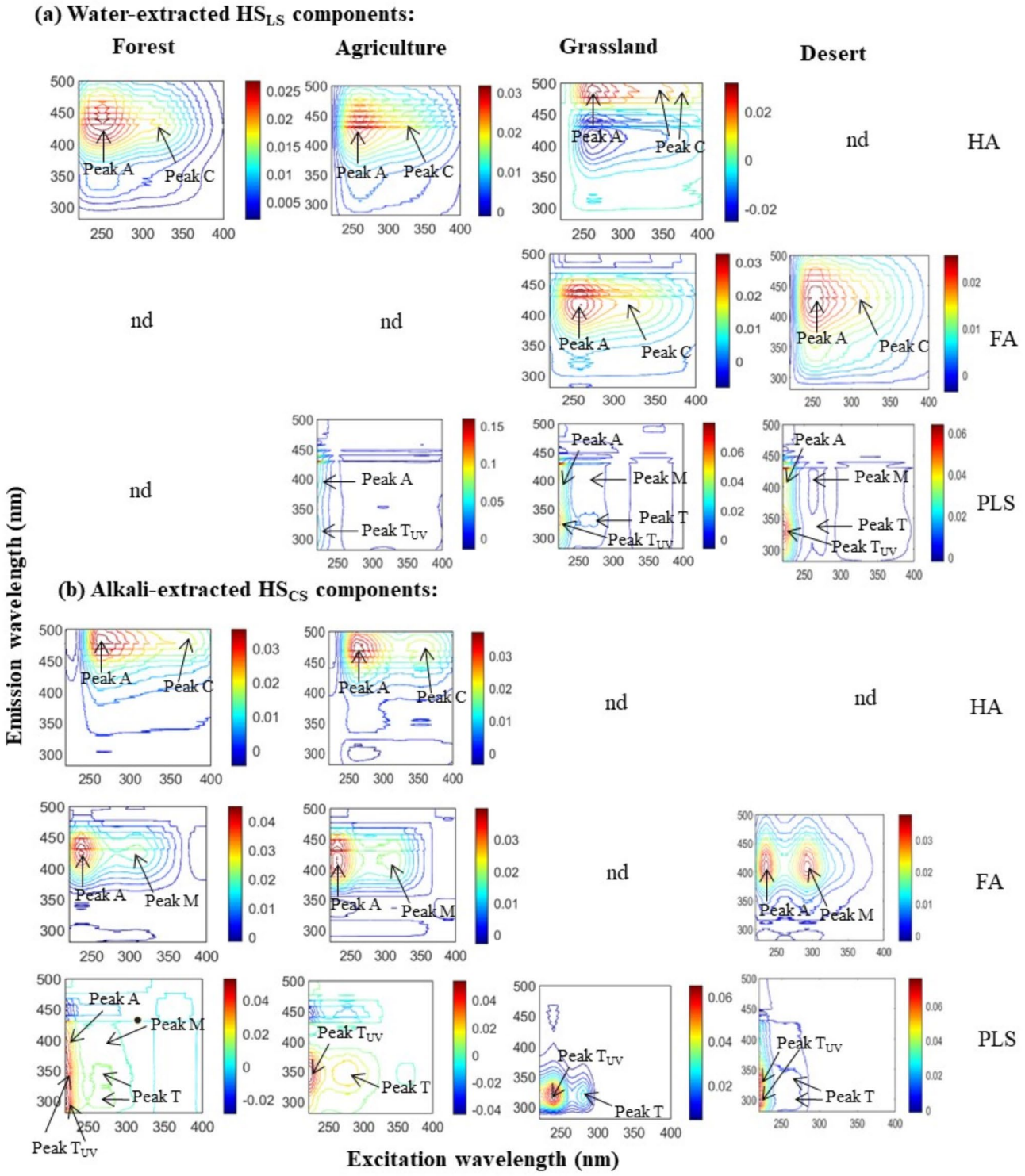

Fig. 6. Fluorescence (excitation-emission matrix, EEM) spectra of water-extracted/labile state (HSLS) (**a**) and alkali-extracted/complexed state (HSCS) (**b**) of humic substances from forest, agriculture, grassland and desert dry-affected soils, and detected fluorescence peaks of humic acid-like (HA-like), fulvic acid-like (FA-like) and protein-like substances-like (PLS-like) identified using EEM-PARAFAC modeling. 'nd': not detected.

peak T_{UV}, 220/351 nm[81,82]. These results suggest that tryptophan-like substances might be secondary derivatives originating from degradation of PLS in agricultural soils by microbial activities[83,84]. The remaining text of this section are presented in the SI.

Discussion

Photosynthetically-derived SOC and pH-dependent SIC or DIC_{LS+CS} sequestration

The significant negative correlation between DIC_{LS} and δ^{13}C-SOC, and the insignificant correlation between DIC_{CS} and δ^{13}C-SOC (Table 2) strongly suggests that SOC primarily arises from inorganic carbon fixation (mostly DIC_{LS}) in drying-affected soil types. Such photosynthetically-derived SOC exports HS components that are mainly responsible for mineral neoformation[54,55], which is further confirmed by the significant negative correlation between δ^{13}C-SOC and $SiO_3^{2-}{}_{CS}$ (Table 2). Further evidence of such photosynthetically-derived SOC is provided by the high variation of δ^{13}C-SOC (-26.93‰ to -21.04‰) among all soils (Table 1), which might derive from uptake of DIC originating from the heterotrophic mineralization of HS components[46,48,85]. With this regard, many studies have found that anoxygenic photosynthesis generally occurs *via* simultaneous carbon and sulfur sequestration by lichen-associated cyanobacterial-fungal symbioses, resulting in COS uptake[13–18]. Further evidence of SOC-associated sulfur sequestration is provided by the significant correlation of δ^{13}C-SOC with both $SO_4^{2-}{}_{CS}$ and $SO_4^{2-}{}_{LS}$ (Table 2).

Most importantly, because of the absence of any plant material in desert soils, newly-derived FA_{LS} and PLS_{LS} (Fig. 6; Table S2) would primarily arise from SOC produced by anoxygenic photosynthesis and/or primary producers[39,40,52,53]. Such anoxygenic photosynthetic activities are further supported by the detection of newly-derived, intact and fresh PLS_{LS+CS} in desert soils (Fig. 6), similar to those found in forest soils[77]. Further support to this interpretation is provided by the occurrence of mineral-bound degraded FA_{CS} and PLS_{CS} as discussed above (Fig. 6; Table S2)[77]. Moreover, desert's FA_{LS} and PLS_{LS} components are absent in either forest or agricultural soils, where plant material-derived FA_{LS} and PLS_{LS} do not form rapidly. In contrast, anoxygenic photosynthetic microorganisms may rapidly produce fresh FA_{LS} and PLS_{LS} as in the case of water and snow environments[82,86]. However, FA_{CS} and PLS_{CS} derived from both plants and anoxygenic photosynthesis would remain in HS_{CS}-bound minerals[36,37,79,87], which implies the stabilization of SOC or HS_{CS} *via* organo-mineral formation in extreme drying-affected soils, except for grassland soils that appear to be highly vulnerable for C stabilization and accumulation *via* organo-mineral complexes. Therefore, anoxygenic photosynthesis in desert soils might contribute DOM or HS through soil microorganisms and generate carbonate minerals *via* sequestration and uptake of DIC_{LS+CS} and COS derived from SOC and DOC mineralization and/or atmospheric COS. These processes would play important roles in reducing CO_2 emissions from soil.

The significant negative correlations of pH with SIC and DIC_{CS}, the significant positive correlations of SIC with SOC, STN, STH, and water contents, and of DIC_{CS} with water contents and SOC (Table 2; Fig. S4a) would suggest a pH-dependent SIC or DIC uptake in the sequestration and fixation of photosynthetically-derived SOC under wet conditions[16,32,88,89]. Furthermore, the significant negative correlation of pH with SOC and DOC_{LS+CS} (Fig. S4b; Table S2) would suggest that high SOC up to a certain acidic pH contributes primarily to all microbial activities due to the relatively low contribution of DOC_{LS+CS} (approximately 1.4–33.6% and, on average, 7.5 ± 7.3% of SOC). High microbial activities at near-neutral pH (5.5–7.5) might be a key factor for the high occurrence of SOC, ascribed to high bacterial diversity and biomass[90,91], due to the high availability of nutrients and HS present in weak (when formed) organo-mineral complexes with metals[90,92,93]. Remarkably, a mild acidic pH would imply soil HS to remain in a non-complexed state, which is further supported by the significant negative correlations of pH with SOC, STN, STH, DOC_{LS+CS}, DIC_{CS}, $NH_4^+{}_{CS}$, $NO_2^-{}_{CS}$, $PO_4^{3-}{}_{CS}$ and DOP_{CS} (Table 2). These results also suggest higher availability of all these components up to acidic pH 5.63[83,94,95], which might be due to intense fungal and bacterial activities[90,91]. Mild acidic-alkaline pH values would lead to high SOC sequestration by lichen-associated cyanobacterial-fungal symbioses[16–18,32,88,89], due to the higher presence of various nutrients plus SIC or DIC[96]. This, in turn, would imply a high heterotrophic SOC mineralization due to the higher presence of bacteria under near-neutral pHs[49,83,97] *via* $SO_4^{2-}{}_{LS+CS}$ reduction during simultaneous sulfur and carbon sequestration. Such simultaneous sequestration-mineralization processes under near-neutral pH conditions would thus lead to the presence of high SIC, SOC and STN contents, together with their dissolved forms such as DIC_{CS}, DOC_{LS+CS}, $NH_4^+{}_{CS}$, $NO_2^-{}_{CS}$, $PO_4^{3-}{}_{CS}$, and DOP_{CS} (Fig. 2; Table 1).

Differently, an increase of pH (> pH 7.5) would primarily result in the formation of strong organo-mineral complexes, which would occur due to the increased presence of anionic forms (e.g. $-COO^-$) of the functional groups in HS components under elevated pH conditions[36,98]. In turn, this process would induce a reduced availability of SIC and most mineral nutrients[96]. These conditions would involve the simultaneous decrease of the diversity of soil bacterial communities and enzymatic activities (Table 2)[99]. Thus, the main effects would include a decrease in sulfate-reducing bacteria[100] due to reduced nutrient availability, which results from increased SOC sequestration and stability under high pH conditions[16,18,88]. Soil C sequestration *via* mineral neoformation is further supported by the significant negative correlation of δ^{13}C-SOC with DIC_{LS}, $NH_4^+{}_{LS}$, $NO_2^-{}_{LS+CS}$, $SiO_3^{2-}{}_{CS}$, and $PO_4^{3-}{}_{LS}$, possibly due to their anoxygenic photosynthetic uptake[13,15–17]. Thus, pH plays an important role in regulating SIC and SOC sequestration-transformation *via* DIC_{LS+CS}, which is primarily controlled by the occurrence of DOC_{LS+CS} and $SiO_3^{2-}{}_{LS+CS}$ in the various soil types examined.

Remarkably, the $SiO_3^{2-}{}_{CS}$-normalized DIC_{LS} and DIC_{CS} values, i.e., the $DIC_{LS}/SiO_3^{2-}{}_{CS}$ and $DIC_{CS}/SiO_3^{2-}{}_{CS}$ ratios showed a significant linear relationship between them (Fig. S4g) whereas the $DIC_{CS}/SiO_3^{2-}{}_{CS}$ ratio varied largely, from 0.2 to 6.0 mg/kg/$SiO_3^{2-}{}_{CS}$ and showed, on average, high and very similar values in forest soils (2.0 ± 2.0 mg/kg/$SiO_3^{2-}{}_{CS}$), grassland soils (1.9 ± 2.1 mg/kg/$SiO_3^{2-}{}_{CS}$), and desert soils (2.1 ± 1.37 mg/kg/$SiO_3^{2-}{}_{CS}$), while the lowest value was found in agricultural soils (0.6 ± 0.5 mg/kg/$SiO_3^{2-}{}_{CS}$). These results would suggest that DIC_{CS} in forest, grassland, and desert soils remains primarily under mineral protection, mostly in carbonate and secondary clay, Fe and LDHs-like minerals. Interestingly, the lowest $DIC_{CS}/SiO_3^{2-}{}_{CS}$ ratios and the highest $DIC_{LS}/SiO_3^{2-}{}_{LS}$ ratios measured in agricultural soils would indicate that the dissolution and mineralization of silicate minerals[19,101,102] might intensively occur during human activities (e.g. ploughing, tilling, and cultivation), thereby resulting the mineralization of DIC_{CS} from minerals and its subsequent export

into DIC_{LS} only in agricultural soils[85]. These results are further supported by the significant negative correlation between pH and $DIC_{CS}/SiO_3^{2-}{}_{LS}$ ratios (Fig. S4j).

Mechanisms of SO_4^{2-}-mediated mineralization of soil biogenic components

The $SO_4^{2-}{}_{LS}$ and $SO_4^{2-}{}_{CS}$ concentrations follow the order: desert soils (respectively, 103.2% and 47.4% higher than grassland soils) > grassland soils (respectively, 45.4% and 212.4% higher than agricultural soils) > agricultural soils (respectively, 96.5% and 10.6% higher than forest soils) > forest soils. In essence, a comprehensive relationship of STS and $SO_4^{2-}{}_{LS+CS}$ with soil biogenic components occur in either solid phase (e.g., SOC, δ^{13}C-SOC, SIC, STN and STH) or liquid phase (e.g. DOC_{LS+CS}, DIC_{LS+CS}, $SiO_3^{2-}{}_{LS+CS}$, $NH_4^{+}{}_{LS+CS}$, $PO_4^{3-}{}_{LS+CS}$ and DOP_{LS+CS}), showing low STS and $SO_4^{2-}{}_{LS+CS}$ contents correlate with high amounts of soil components in the solid and liquid phases for all soil type, and vice versa (Figs. 3 and 5). These results imply that intense redox activities would arise from sulfur and carbon sequestration by COS and/or H_2S uptake[28,57,103] through sequestration ($S^{2-} \leftrightarrow S^0$) and reduction-oxidation (redox: $S^0 \leftrightarrow SO_4^{2-} \leftrightarrow S^{2-}/S_2^{2-} \leftrightarrow SO_4^{2-}$)[28–30] by lichen-associated cyanobacterial-fungal symbioses[14–17,28,104]. Specifically, significant positive correlations of $SO_4^{2-}{}_{LS}$ and $SO_4^{2-}{}_{CS}$ with δ^{13}C-SOC (Table 2; Fig. 3c) indicates the occurrence of aforementioned C and S sequestration which simultaneously maintains STS via SO_4^{2-} redox processes.

Transformations mediated by SO_4^{2-} are further supported by the following results. First, Principal Component Analysis (PCA) of the solid- and liquid-phase components has revealed the existence of significant consistent associations of negative loadings of STS, $SO_4^{2-}{}_{LS}$ $SO_4^{2-}{}_{CS}$, δ^{12}C-SOC, $NO_3^{-}{}_{LS}$, $NO_3^{-}{}_{CS}$ and pH with positive loadings of SOC, SIC, STN, STH, DOC_{LS}, DOC_{CS}, DIC_{LS}, DIC_{CS}, $NH_4^{+}{}_{LS}$, $NH_4^{+}{}_{CS}$ and water content for PC1, which accounts for the highest variability (47.3%; Table 3). These results suggested that SO_4^{2-} reduction was very relevant in enhancing the sequestration of both inorganic and organic C and N in the growth of photosynthetic soil microorganisms under conditions of high water availability and low pH. Concurrently this process would also facilitate the release of DOC, DIC, and NH_4^+. The observed increased sequestration of C and N was further supported by the analysis of PC2, which indicated that the positive loadings of SOC, δ^{12}C-SOC, STN, STH, STS, $SO_4^{2-}{}_{LS}$ and $SO_4^{2-}{}_{CS}$ were associated to the uptake of DIC_{LS}, $SiO_3^{2-}{}_{LS}$ and $SiO_3^{2-}{}_{CS}$, as indicated by their negative loadings (Table 3). Furthermore, the occurrence of C sequestration, along with the stability of organo-mineral and carbonate mineral, was supported by the significant negative loadings of δ^{12}C-SOC associated to the significant positive loadings of DOC_{CS} and DIC_{CS}, as indicated by PC3 and PC5 (Table 1). In conclusion, the

Variables	PC1	PC2	PC3	PC4	PC5
pH	-0.238	-0.132	0.132	-0.094	0.363
Water content	0.253	0.168	0.088	-0.112	-0.203
SOC	0.275	0.172	0.047	-0.098	-0.019
STN	0.235	0.200	0.001	0.063	-0.174
STH	0.244	0.251	0.109	-0.008	-0.032
STS	-0.142	0.299	0.253	0.105	0.201
δ^{13}C-SOC	-0.168	0.175	-0.309	-0.058	-0.243
SIC	0.230	0.195	0.120	0.012	-0.294
Sand	-0.163	-0.132	0.284	-0.505	-0.207
Silt	0.141	0.152	-0.287	0.525	0.228
Clay	0.207	-0.136	-0.048	-0.062	-0.122
$SO_4^{2-}{}_{LS}$	-0.219	0.253	0.093	0.160	0.118
$SO_4^{2-}{}_{CS}$	-0.201	0.261	0.202	0.119	0.152
DOC_{LS}	0.290	0.066	0.139	0.018	0.026
DOC_{CS}	0.245	-0.121	0.236	0.052	0.276
DIC_{LS}	0.112	-0.384	0.182	0.166	0.099
DIC_{CS}	0.197	-0.035	0.109	-0.256	0.469
$NH_4^{+}{}_{LS}$	0.260	0.137	0.107	-0.096	0.165
$NH_4^{+}{}_{CS}$	0.259	0.114	0.072	-0.059	0.064
$NO_3^{-}{}_{LS}$	-0.175	0.142	0.395	0.162	-0.201
$NO_3^{-}{}_{CS}$	-0.172	0.163	0.435	0.141	-0.116
$SiO_3^{2-}{}_{LS}$	0.047	-0.317	0.127	0.432	-0.219
$SiO_3^{2-}{}_{CS}$	0.131	-0.354	0.272	0.188	-0.152
Eigenvalue	10.89	4.42	2.02	1.54	0.99
Variability (%)	47.3	19.2	8.8	6.7	4.3
Cumulative (%)	47.3	66.5	75.3	82.0	86.3

Table 3. Loadings of soil component parameters on five significant principal component variables and total variance explained, for samples collected from four drying-affected soil types (forest, agriculture, grassland, and desert) in the Xinjiang Uyghur autonomous region, China.

results described above indicated the simultaneous occurrence of sequestration and $SO_4^{2-}{}_{CS}$ reduction, which are consistent with results of previous studies[16,28,89,96,103,105,106].

Second, results from an experimental study conducted on a forest haplic luvisol have demonstrated that the sequestration of C, N, and S by soil microorganisms might occur simultaneously during their growth and metabolism, and result in a net increase of STS (1.2–41.0%) and STN (1.7–7.0%) under sunlight, dark, and control conditions during the incubation periods of 0, 30, 75, and 150 days[34]. However, C sequestration was not consistently detected due to the simultaneous offsets of photochemical and microbial respiration, which led to a significant loss of SOC. In particular, a net increase of SOC was measured only under sunlight (0.80%) and control (0.40%) conditions during the 75–150 day period following mineralization, whereas a decrease from 1.8 to 2.4% and from 2.3 to 6.0% respectively, was measured during the initial 0–75 days[34].

Finally, a similar sequestration of C, N and S, together with SO_4^{2-}-mediated transformations, have been measured in various soils and desert sands of Inner Mongolia, for which significant positive correlations of STS with SOC and STN, and significant negative correlations with δ^{13}C-SOC (ranging from −24.9‰ to -7.10‰) were observed[96].

Such photosynthetic S and C fixation by microorganisms is substantially stimulated in wet conditions[104–106] and is the only primary way by which they conserve their energy, diversity, and biomass from sulfide oxidation in desert soils[104,107]. In parallel, the eight electrons released from the redox reactions ($S^{2-]} \rightarrow S^O + 2e^-$ and $S^O \rightarrow SO_4^{2-} + 6e^-$)[30] would generate reactive oxygen species and trigger export of soil components from the mineralization/dissolution of various minerals[83,90,108,109]. Moreover, the linear positive relationships of both $NO_3^-{}_{LS}$ and $NO_3^-{}_{CS}$ with STS, $SO_4^{2-}{}_{LS}$, and $SO_4^{2-}{}_{CS}$ would suggest a simultaneous occurrence of both nitrification and denitrification[62–64]. Furthermore, the DOC_{LS+CS} mineralization[33] determines the export of several soil components (e.g. DIC_{LS+CS}, $NH_4^+{}_{LS+CS}$, SiO_{3LS+CS}, etc.) by mineral dissolution[31,35,56,69], as well as of DIC_{LS+CS} and $NH_4^+{}_{LS+CS}$ from DOC_{LS+CS} mineralization[25,66,82] *via* $SO_4^{2-}{}_{LS+CS}$ reduction. In particular, the $SO_4^{2-}{}_{LS}$-normalized DOC_{LS} and DOC_{CS} show relatively higher contents (0.3–3100 and 1.1–14800 g/kg/$SO_4^{2-}{}_{LS}$, respectively) compared to the corresponding $SO_4^{2-}{}_{CS}$-normalized DOC_{LS} and DOC_{CS} values (0.16–570 and 0.52–5900 g/kg/$SO_4^{2-}{}_{CS}$, respectively). Very similar results are obtained for DIC_{LS} and DIC_{CS} (0.6–1900 and 1.4–9400 g/kg/$SO_4^{2-}{}_{LS}$), which are respectively higher than 0.3–1000 and 0.7–3000 g/kg/$SO_4^{2-}{}_{CS}$, and for $SiO_3^{2-}{}_{LS}$ and $SiO_3^{2-}{}_{CS}$ (1.6–1700 and 0.2–5100 g/kg/$SO_4^{2-}{}_{LS}$, respectively, higher than 0.8–1500 and 0.1–4900 g/kg/$SO_4^{2-}{}_{CS}$), as well as for other components (Fig. 3). These effects are presumably due to the occurrence of mineralization and respiration at the mineral-microbes/organic interface[31,32] or of CS forms in soils[33], which subsequently cause the export of soil components in LS-forms (Fig. 7). These results would indicate that $SO_4^{2-}{}_{LS+CS}$-mediated redox processes[28,29,57] primarily lead to the dissolution of HS-associated clay, Fe, and LDHs-like minerals, so that the existing organo-mineral soil components would remain in a degraded state under the existing environmental factors and conditions[77,110] after undergoing mineralization by $SO_4^{2-}{}_{LS+CS}$-mediated microbial heterotrophic respiration[28,29,49,57]. The soil $SO_4^{2-}{}_{LS+CS}$ contents ultimately lead to control the mineral-associated soil components as depicted in the conceptual model shown in Fig. 7.

Apparently, the SOC production by anoxygenic photosynthesis in desert soils[39,40,53] and by decay of from plant-derived litter materials[47,48] and subsequent mineralization by $SO_4^{2-}{}_{LS+CS}$ and/or STS could be a common unique feature of all soil types (Figs. 3 and 5). The transformation (e.g., mineralization or neoformation) of soil components *via* SO_4^{2-} reduction leads to the subsequent export of components in LS, CS, and mineral forms (Fig. 7) to ambient environments through rainwater and water discharge. These processes would suggest that $SO_4^{2-}{}_{LS+CS}$–mediated redox reactions are the key controlling factors for the dissolution of clay, Fe and LDHs-like minerals, and for maintaining all soil components in steady state with $SO_4^{2-}{}_{LS+CS}$ and STS.

Signals of soil desertification and salinization

The degradative steady state of SOC, SIC, STN, and STH in the various examined soils, due to STS-mediated transformation, is primarily responsible for the coherent transformation of SOM[77,110]. The occurrence of this degradative state is further supported by the corresponding dissolved-phase components (which include DOC_{LS+CS}, DIC_{LS+CS}, $SiO_3^{2-}{}_{LS+CS}$, $NH_4^+{}_{LS+CS}$, $NO_2^-{}_{LS+CS}$, $PO_4^{3-}{}_{LS+CS}$, and DOP_{LS+CS}), and by the $SO_4^{2-}{}_{LS+CS}$-mediated heterotrophic respiration in the soil matrix[28,29,49,57]. Such solid-phase and liquid-phase transformations clearly suggest that STS *via* $SO_4^{2-}{}_{LS+CS}$ reduction-oxidation (redox) processes[28,29,57] are key factors in regulating the relevant soil components. Such transformations would induce degradation of mineral-associated SOC and DOC_{LS+CS}, and simultaneously produce DIC_{LS+CS} and other nutrients. The continuous degradation of SOC without input from decaying plant materials[46–48] leads to increasing SIC *via* inorganic carbonate mineral neoformation[21–23,51]. This process unveils the highest contents of STS and $SO_4^{2-}{}_{LS+CS}$ at low contents of SOC and nutrients, which might initiate desertification.

Remarkably, the repeated occurrence of sulfide-dependent anoxygenic and oxygenic photosynthetic sulfur and carbon sequestration through COS uptake[18] by lichen-associated cyanobacterial-fungal symbioses[14–17,104] causes accumulation of S° with the simultaneous transfer to SO_4^{2-} by soil fungi and bacteria[28]. In particular, desert soils feature a significant CO_2/DIC uptake via photosynthetic microorganisms and, possibly, SOC-associated mineral formation[39,40,52,53]. Notably, high SO_4^{2-} contents are often detected in saline-alkali soils that are usually denoted as sulfate-type saline soil[24,26,27]. Therefore, high contents of STS and/or $SO_4^{2-}{}_{LS+CS}$ in one forest soil and one agricultural soil, three grassland soils, and all desert soils would represent the prime signature of increasing salinity and desertification.

Materials and methods

Soil sampling sites, collection, and Preparation

The studied soils were collected from the Xinjiang Uygur Autonomous Region located in the northwest part of China, i.e., the central part of Eurasia (73°40′–96°23′E longitude and 34°25′–49°10′N latitude), which covers an

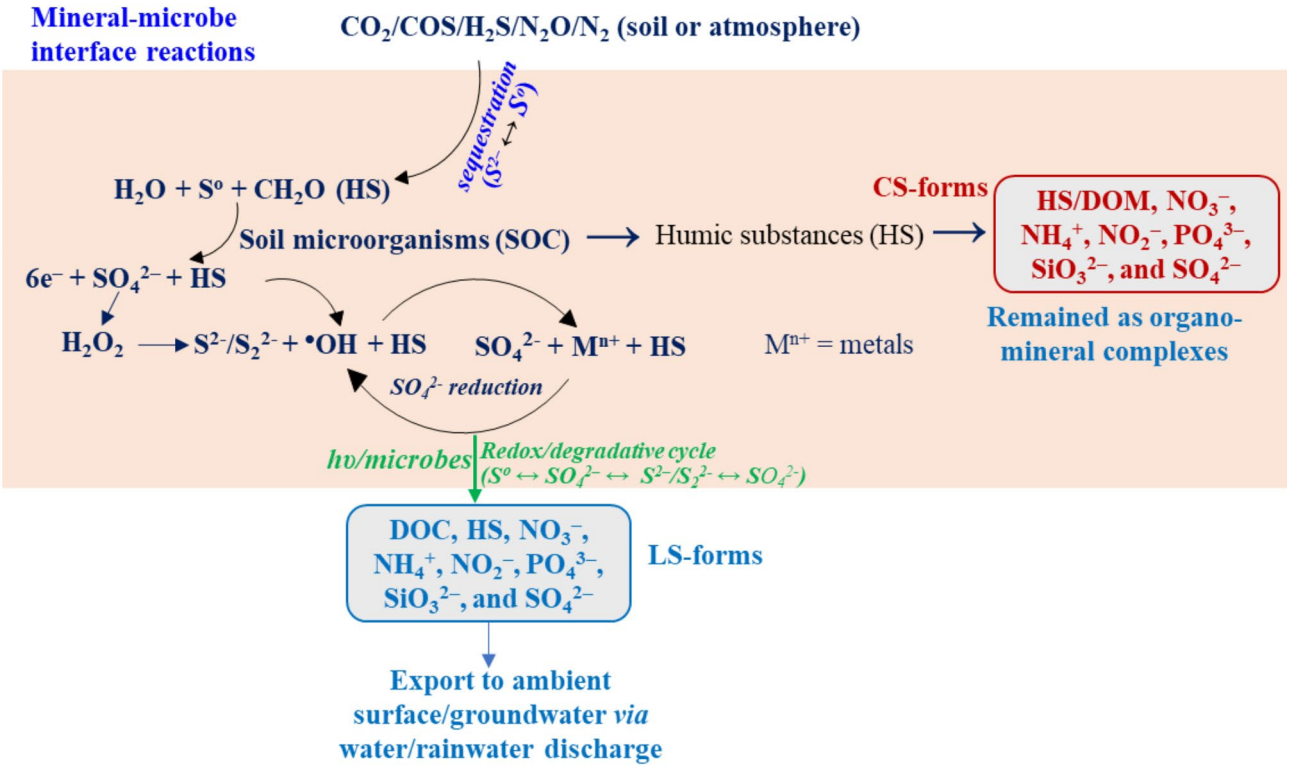

Fig. 7. A conceptual model for the sequestration of C, S, and N, which highlights the simultaneous maintenance of sequestration ($S^{2-} \leftrightarrow S°$) and reduction-oxidation (redox: $S° \leftrightarrow SO_4^{2-} \leftrightarrow S^{2-}/S_2^{2-} \leftrightarrow SO_4^{2-}$) processes by soil microorganisms during the transformation of organo-mineral components in the drying-affected soils. This leads to the exports of their LS-forms (DOC_{LS}, HS_{LS}, $NO_{3\ LS}^-$, $NH_{4\ LS}^+$, $NO_{2\ LS}^-$, $PO_{4\ LS}^{3-}$, $SiO_{3\ LS}^{2-}$ and $SO_{4\ LS}^{2-}$) and mineral neoformation of their CS-forms (DOC_{CS}/HS_{CS}, $NO_{3\ CS}^-$, $NH_{4\ CS}^+$, $NO_{2\ CS}^-$, $PO_{4\ CS}^{3-}$, $SiO_{3\ CS}^{2-}$ and $SO_{4\ CS}^{2-}$).

area of more than 1.66 million km^2 that makes Xinjiang the largest province in China. The mountainous area includes hills and plateaus for approximately 800,000 km^2, and the plain area includes the intermountain Tarim and Junggar Basins for approximately 800,000 km^2. The climate of Xinjiang is temperate continental with a long winter (mid-Oct-Mar) and a relatively short summer (May–Aug). The air temperature is largely fluctuating showing the highest value of 41.0 °C and the lowest one of − 28 °C (Table S1). Xinjiang is an arid area featuring small and uneven annual precipitations that ranged from 74.0 to 409 mm since 2012, showing the lowest value in 2022 and the highest in 2015 (Table S1).

The land use/cover of Xinjiang includes six categories: cultivated and arable land (5.5%); forest land (1.68%); grassland (29.5%); water area (2.1%), construction land (0.6%), and unused land (60.5%)[114]. More than half of soils in Xinjiang consist of sandy, desert (Gobi), saline-alkaline, bare soils and bare rocks. The mountainous area is more extended than the plain one, and the northern area is more extended than the southern one. The dominant forest tree species is *populus Euphratica*, and forest types include valley secondary forest and plain artificial forest. The ecological green component of forest land, grassland and cultivated land accounts for just 37.2% of the total land area of Xinjiang. This indicates that its ecological and environmental quality is not high, the system resistance is not strong, and the ecosystem is fragile.

In this work a total of 20 soil samples, i.e., 5 under forest, 4 from agricultural land, 6 from grassland, and 5 from desert were collected near Urumqi City, (Fig. S1), in a sampling area ranging from N 42°31′04″–N 45°27′36″, E 86°17′34″4–E 88°20′51″.

The forest soils were collected under coniferous species located near the slum areas of Urumqi. The grassland soils were mostly collected from artificial grassland and scattered in Urumqi and its surrounding areas. The desert soils were characterized by the absence of vegetation cover and high sand content, and some are red soils in sandy areas. The agricultural soils were collected from soybean, rape, and corn fields.

Samples were randomly collected from the soil top layer (~ 0–15 cm) after removing grasses and debris, using a 10-cm diameter stainless steel auger as described previously[77]. After removing manually plant litters, roots, and debris, each sample was mixed homogeneously to obtain a spatially representative sample at the field scale. Soil samples were then oven dried at 40 °C[77], passed through a 2-mm sieve, ground in a mortar to obtain particle sizes lower than 0.2 mm, and stored at -20 °C until further use.

Water and alkaline extracts of soil samples

Soil HS were isolated using a novel method[77] based on the extraction with water first, followed by a 0.1 M NaOH solution. The two extracts were obtained by several subsequent steps (Fig. S1). In the first step, ultrapure water (18.2 MΩ·cm, Mill-Q, Millipore) was added to each ground and sieved soil sample at a 1:10 soil/water ratio, the mixture was vortexed for 1 min in closed 500-mL brown bottles, and then shaken for 6 h at 25 °C. Afterwards, it was centrifuged for 20 min at 4000 rpm using a Thermo Fisher Scientific SORVALL ST 16 centrifuge, to remove suspended solids. The supernatant solution was then filtered through a 0.45-µm membrane filter (GF/F type, Shanghai Xin Ya Purification Equipment Co. Ltd, China), whereas the remaining solid residue was extracted again with fresh ultrapure water for 1 h. The above procedure was applied again to obtain a supernatant solution that was mixed with the previous one and stored in freezer at −20 °C until further processing. This solution represents the soil water extract (W_e).

In the second step, the soil residue after water extraction was subjected to alkaline extraction under N_2 with a 0.1 M NaOH solution, at 1:10 soil residue/alkaline solution ratio, by shaking for 3 h at 25 °C. The mixture was then centrifuged as described above and the supernatant solution filtered through a 0.45-µm membrane filter (polytetrafluoroethylene membrane, PTFE, Shanghai Xin Ya Purification Equipment Co. Ltd, China). The remaining solid residue was extracted again with a fresh alkaline solution for 3 h, and the procedure described above was applied again to obtain another supernatant solution that was mixed with the previous one to obtain the alkaline extract (A_e), and stored in freezer at −20 °C until further processing.

The W_e and A_e samples represent, respectively, the water-extracted (labile state, LS) components (DOM/DOC_{LS}, HS_{LS}, $NO_3^-{}_{LS}$, $NH_4^+{}_{LS}$, $NO_2^-{}_{LS}$, $PO_4^{3-}{}_{LS}$, $SiO_3^{2-}{}_{LS}$ and $SO_4^{2-}{}_{LS}$) and the alkali-extracted (complexed state, CS) components (correspondingly, DOC_{CS}, HS_{CS}, $NO_3^-{}_{CS}$, $NH_4^+{}_{CS}$, $NO_2^-{}_{CS}$, $PO_4^{3-}{}_{CS}$, $SiO_3^{2-}{}_{CS}$, and $SO_4^{2-}{}_{CS}$).

All glass bottles used for extraction purposes were soaked with 10% HNO_3 and HCl for 24 h before use, rinsed with Mill-Q (MQ) water, and then placed in a muffle furnace for 4 h at 550 °C in order to remove residual organic matter. Similarly, each glass fiber filter was individually wrapped in an aluminum foil and then placed in a muffle furnace for 4 h at 550 °C, in order to remove any organic and inorganic impurities.

Analytical methods

Soil particle size was measured on the 2-mm size soil fraction using the hydrometer method (Mastersizer 3000, Malvern). Soil water extracts were directly used for all analytical measurements (DOC, nutrients, fluorescence), whilst alkaline extracts were previously adjusted to approximately pH 8.0 before measurements. The DOC and DIC contents in W_e and A_e samples were measured in triplicate by injection of each sample into an Aurora combustion total organic carbon (TOC) analyzer equipped with autosampler (O.I. Analytical Aurora-Model 1030 W, USA). The pH and EC were measured in a 1:2.5 soil residue/ultrapure water solution ratio, using a pH meter (Multi 3630 IDS, Germany) equipped with a combination electrode.

Nutrients, including total phosphorus (TP), phosphates (PO_4^{3-}), total nitrogen (TN), nitrates (NO_3^-), nitrites (NO_2^-), ammonium (NH_4^+), and silicates (SiO_3^{2-}), were determined in W_e and A_e using an automated continuous flow analyzer system (SKALAR San++, Netherlands).

Soil total carbon (STC), soil total nitrogen (STN), soil total sulfur (STS) and soil total hydrogen (STH) were measured with a Vario EL Cube Elemental Analyzer (Elementar VarioEL III, Germany) on approximately 20-mg aliquots of dried, ground and homogenized sample contained into a clean, carbon-free pre-combusted tin boat placed in the autosampler rack assembly. Soil organic carbon (SOC) was analyzed by an Elemental Analyzer described elsewhere[76] on dried, ground, and homogenized samples pretreated with 1 M HCl, which were contained in vials in the autosampler tray. Sulfanilamide was used as standard after every 10 measurements. Soil inorganic carbon (SIC) was obtained as SIC = STC - SOC. The stable ^{13}C isotope was analyzed by an Elemental Analyzer (Flash 2000 HT) interfaced with a stable carbon isotope ratio mass spectrophotometer (MAT 253 PlusTM, ThermoFisher, USA) on each soil sample, prepared as described above and placed in a IAEA-600 autosampler rack assembly, using caffeine as the ^{13}C standard.

The remaining text of site description, water and alkaline extracts of soil samples, analytical methods (fluorescence spectra and PARAFAC model), and statistical analyses are discussed in the supplementary information.

Data availability

The authors declare that the data supporting the findings of this study are available within the paper and its supplementary information files.

Received: 27 October 2024; Accepted: 18 March 2025
Published online: 21 March 2025

References

1. Wang, L. X. et al. Dryland productivity under a changing climate. *Nat. Clim. Chang.* **12**, 981–994. https://doi.org/10.1038/s41558-022-01499-y (2022).
2. Delgado-Baquerizo, M. et al. Decoupling of soil nutrient cycles as a function of aridity in global drylands. *Nature* **502**, 672–676. https://doi.org/10.1038/nature12670 (2013).
3. Poulter, B. et al. Contribution of semi-arid ecosystems to interannual variability of the global carbon cycle. *Nature* **509**, 600–603. https://doi.org/10.1038/nature13376 (2014).
4. Reynolds, J. F. et al. Global desertification: Building a science for dryland development. *Science* **316**, 847–851. https://doi.org/10.1126/science.1131634 (2007).
5. Homyak, P. M., Allison, S. D., Huxman, T. E., Goulden, M. L. & Treseder, K. K. Effects of drought manipulation on soil nitrogen cycling: A meta-analysis. *J. Geophys. Res. Biogeosci.* **122**, 3260–3272. https://doi.org/10.1002/2017JG004146 (2017).

6. Huang, J. P., Yu, H. P., Guan, X. D., Wang, G. Y. & Guo, R. X. Accelerated dryland expansion under climate change. *Nat. Clim. Chang.* **6**, 166–. https://doi.org/10.1038/NCLIMATE2837 (2016).
7. Lal, R. Carbon cycling in global drylands. *Curr. Clim. Chang. Rep.* **5**, 221–232. https://doi.org/10.1007/s40641-019-00132-z (2019).
8. Li, C. J. et al. Drivers and impacts of changes in China's drylands. *Nat. Rev. Earth Environ.* **2**, 858–873. https://doi.org/10.1038/s43017-021-00226-z (2021).
9. Gao, D. C. et al. Responses of soil nitrogen and phosphorus cycling to drying and rewetting cycles: A meta-analysis. *Soil. Biol. Biochem.* **148** https://doi.org/10.1016/j.soilbio.2020.107896 (2020).
10. Leizeaga, A., Meisner, A., Rousk, J. & Baath, E. Repeated drying and rewetting cycles accelerate bacterial growth recovery after rewetting. *Biol. Fertil. Soils.* **58**, 365–374. https://doi.org/10.1007/s00374-022-01623-2 (2022).
11. Barnard, R. L., Blazewicz, S. J. & Firestone, M. K. Rewetting of soil: Revisiting the origin of soil CO_2 emissions. *Soil. Biol. Biochem.* **147** https://doi.org/10.1016/j.soilbio.2020.107819 (2020).
12. Manzoni, S. et al. Rainfall intensification increases the contribution of rewetting pulses to soil heterotrophic respiration. *Biogeosciences* **17**, 4007–4023. https://doi.org/10.5194/bg-17-4007-2020 (2020).
13. Diaz, M. A. et al. Stable isotopes of nitrate, sulfate, and carbonate in soils from the transantarctic mountains, Antarctica: A record of atmospheric deposition and chemical weathering. *Front. Earth Sci.* **8** https://doi.org/10.3389/feart.2020.00341 (2020).
14. Asaf, D. et al. Ecosystem photosynthesis inferred from measurements of carbonyl sulphide flux. *Nat. Geosci.* **6**, 186–190. https://doi.org/10.1038/ngeo1730 (2013).
15. Cohen, Y., JØrgensen, B. B., Padan, E. & Shilo, M. Sulphide-dependent anoxygenic photosynthesis in the Cyanobacterium oscillatoria limnetica. *Nature* **257**, 489–492. https://doi.org/10.1038/257489a0 (1975).
16. Heckman, D. S. et al. Molecular evidence for the early colonization of land by fungi and plants. *Science* **293**, 1129–1133. https://doi.org/10.1126/science.1061457 (2001).
17. Loron, C. C. et al. Early fungi from the proterozoic era in Arctic Canada. *Nature* **570**, 232–235. https://doi.org/10.1038/s41586-019-1217-0 (2019).
18. Protoschill-Krebs, G. & Kesselmeier, J. Enzymatic pathways for the consumption of carbonyl sulphide (COS) by higher plants*. *Bot. Acta.* **105**, 206–212. https://doi.org/10.1111/j.1438-8677.1992.tb00288.x (1992).
19. Naorem, A. et al. Soil inorganic carbon as a potential sink in carbon storage in dryland soils-a review. *Agriculture-Basel* **12** https://doi.org/10.3390/agriculture12081256 (2022).
20. Diaz-Hernandez, J. L. Is soil carbon storage underestimated? *Chemosphere* **80**, 346–349. https://doi.org/10.1016/j.chemosphere.2010.04.038 (2010).
21. Liu, Z. et al. Soil microbes from saline-alkali farmland can form carbonate precipitates. *Agronomy-Basel* **13** https://doi.org/10.3390/agronomy13020372 (2023).
22. Ferdush, J. & Paul, V. A review on the possible factors influencing soil inorganic carbon under elevated CO_2. *Catena* **204** https://doi.org/10.1016/j.catena.2021.105434 (2021).
23. Qin, C. Q. et al. Vertical variations of soil carbon under different land uses in a karst critical zone observatory (CZO), SW China. *Geoderma* **412** https://doi.org/10.1016/j.geoderma.2022.115741 (2022).
24. Zhuang, Q. W. et al. Evolution of soil salinization under the background of landscape patterns in the irrigated Northern slopes of Tianshan mountains, Xinjiang, China. *Catena* **206** https://doi.org/10.1016/j.catena.2021.105561 (2021).
25. Zhang, Y. T. et al. Photo-ammonification of low molecular weight dissolved organic nitrogen by direct and indirect photolysis. *Sci. Total Environ.* **764** https://doi.org/10.1016/j.scitotenv.2020.142930 (2021).
26. Nan, L. L., Guo, Q. A. N. & Cao, S. Y. Archaeal community diversity in different types of saline-alkali soil in arid regions of Northwest China. *J. Biosci. Bioeng.* **130**, 382–389. https://doi.org/10.1016/j.jbiosc.2020.06.001 (2020).
27. Nan, L. L., Guo, Q. N., Cao, S. Y. & Zhan, Z. B. Diversity of bacterium communities in saline-alkali soil in arid regions of Northwest China. *BMC Microbiol.* **22**. https://doi.org/10.1186/s12866-021-02424-7 (2022).
28. Lovley, D. R. Bug juice: Harvesting electricity with microorganisms. *Nat. Rev. Microbiol.* **4**, 497–508. https://doi.org/10.1038/nrmicro1442 (2006).
29. Jørgensen, B. B. Mineralization of organic matter in the sea bed—the role of sulphate reduction. *Nature* **296**, 643–645. https://doi.org/10.1038/296643a0 (1982).
30. Huang, M. et al. Mechanism of metal sulfides accelerating Fe(II)/Fe(III) redox cycling to enhance pollutant degradation by persulfate: Metallic active sites vs. reducing sulfur species. *J. Hazard. Mater.* **404** https://doi.org/10.1016/j.jhazmat.2020.124175 (2021).
31. Kleber, M. et al. Dynamic interactions at the mineral-organic matter interface. *Nat. Rev. Earth Environ.* **2**, 402–421. https://doi.org/10.1038/s43017-021-00162-y (2021).
32. Possinger, A. R. et al. Organo–organic and organo–mineral interfaces in soil at the nanometer scale. *Nat. Commun.* **11**, 6103. https://doi.org/10.1038/s41467-020-19792-9 (2020).
33. Fang, C. M., Smith, P., Moncrieff, J. B. & Smith, J. U. Similar response of labile and resistant soil organic matter pools to changes in temperature. *Nature* **433**, 57–59. https://doi.org/10.1038/nature03138 (2005).
34. Mohinuzzaman, M. et al. CQ. Sequestration and transformation of soil components under simulated warming. Manuscript in preparation (will be submitted soon). (2025).
35. Alessi, D. S. et al. The product of microbial uranium reduction includes multiple species with U(IV)–phosphate coordination. *Geochim. Cosmochim. Acta.* **131**, 115–127. https://doi.org/10.1016/j.gca.2014.01.005 (2014).
36. Zhang, J. et al. Isolation of dissolved organic matter from aqueous solution by precipitation with FeCl3: Mechanisms and significance in environmental perspectives. *Sci. Rep.* **13** https://doi.org/10.1038/s41598-023-31831-1 (2023).
37. Kirsten, M. et al. Iron oxides and aluminous clays selectively control soil carbon storage and stability in the humid tropics. *Sci. Rep.* **11**, 5076. https://doi.org/10.1038/s41598-021-84777-7 (2021).
38. Khan, A. I. & O'Hare, D. Intercalation chemistry of layered double hydroxides: Recent developments and applications. *J. Mater. Chem.* **12**, 3191–3198. https://doi.org/10.1039/B204076J (2002).
39. Schlesinger, W. H. An evaluation of abiotic carbon sinks in deserts. *Global Chang. Biol.* **23**, 25–27. https://doi.org/10.1111/gcb.13336 (2017).
40. Liu, Z. et al. Desert soil sequesters atmospheric CO_2 by microbial mineral formation. *Geoderma* **361** https://doi.org/10.1016/j.geoderma.2019.114104 (2020).
41. Lerch, T. Z., Nunan, N., Dignac, M. F., Chenu, C. & Mariotti, A. Variations in microbial isotopic fractionation during soil organic matter decomposition. *Biogeochemistry* **106**, 5–21. https://doi.org/10.1007/s10533-010-9432-7 (2011).
42. Graven, H., Keeling, R. F. & Rogelj, J. Changes to carbon isotopes in atmospheric CO_2 over the industrial Era and into the future. *Global Biogeochem. Cycles* **34**, e2019GB006170 (2020). https://doi.org/10.1029/2019GB006170
43. Wang, G. et al. Paleovegetation reconstruction using δ13C of soil organic matter. *Biogeosciences* **5**, 1325–1337. https://doi.org/10.5194/bg-5-1325-2008 (2008).
44. Huang, W. J. & Hall, S. J. Elevated moisture stimulates carbon loss from mineral soils by releasing protected organic matter. *Nat. Commun.* **8** https://doi.org/10.1038/s41467-017-01998-z (2017).
45. Melillo, J. M. et al. Long-term pattern and magnitude of soil carbon feedback to the climate system in a warming world. *Science* **358**, 101–105 (2017).

46. Vidal, A. et al. Visualizing the transfer of organic matter from decaying plant residues to soil mineral surfaces controlled by microorganisms. *Soil. Biol. Biochem.* **160** https://doi.org/10.1016/j.soilbio.2021.108347 (2021).
47. Craig, M. E. et al. Fast-decaying plant litter enhances soil carbon in temperate forests but not through microbial physiological traits. *Nat. Commun.* **13**, 1229. https://doi.org/10.1038/s41467-022-28715-9 (2022).
48. Islam, M. R., Singh, B. & Dijkstra, F. A. Stabilisation of soil organic matter: Interactions between clay and microbes. *Biogeochemistry* **160**, 145–158. https://doi.org/10.1007/s10533-022-00956-2 (2022).
49. Bond-Lamberty, B. & Thomson, A. Temperature-associated increases in the global soil respiration record. *Nature* **464**, 579–582. https://doi.org/10.1038/nature08930 (2010).
50. Bond-Lamberty, B., Bailey, V. L., Chen, M., Gough, C. M. & Vargas, R. Globally rising soil heterotrophic respiration over recent decades. *Nature* **560**, 80–83. https://doi.org/10.1038/s41586-018-0358-x (2018).
51. Wang, X. J. et al. Carbon accumulation in arid croplands of Northwest China: Pedogenic carbonate exceeding organic carbon. *Sci. Rep.* **5** https://doi.org/10.1038/srep11439 (2015).
52. Yang, F. et al. Evaluation of carbon sink in the Taklimakan desert based on correction of abnormal negative CO_2 flux of IRGASON. *Sci. Total Environ.* **838** https://doi.org/10.1016/j.scitotenv.2022.155988 (2022).
53. Wohlfahrt, G., Fenstermaker, L. F. & Arnone, J. A. Large annual net ecosystem CO_2 uptake of a Mojave desert ecosystem. *Global Chang. Biol.* **14**, 1475–1487. https://doi.org/10.1111/j.1365-2486.2008.01593.x (2008).
54. Lucas, Y. The role of plants in controlling rates and products of weathering: Importance of biological pumping. *Annu. Rev. Earth Planet. Sci.* **29**, 135–163. https://doi.org/10.1146/annurev.earth.29.1.135 (2001).
55. Li, Z., Cornelis, J. T., Linden, C. V., Van Ranst, E. & Delvaux, B. Neoformed aluminosilicate and phytogenic silica are competitive sinks in the silicon soil–plant cycle. *Geoderma* **368**, 114308. https://doi.org/10.1016/j.geoderma.2020.114308 (2020).
56. Trave, A., Selloni, A., Goursot, A., Tichit, D. & Weber, J. First principles study of the structure and chemistry of Mg-based hydrotalcite-like anionic clays. *J. Phys. Chem. B.* **106**, 12291–12296. https://doi.org/10.1021/jp026339k (2002).
57. McRose, D. L. & Newman, D. K. Redox-active antibiotics enhance phosphorus bioavailability. *Science* **371**, 1033–1038. https://doi.org/10.1126/science.abd1515 (2021).
58. Germida, J. J. & Janzen, H. H. Factors affecting the oxidation of elemental sulfur in soils. *Fertilizer Res.* **35**, 101–114. https://doi.org/10.1007/BF00750224 (1993).
59. Li, X. S. et al. Oxidation of elemental sulfur by fusarium Solani strain THIF01 harboring endobacterium Bradyrhizobium Sp. *Microb. Ecol.* **60**, 96–104. https://doi.org/10.1007/s00248-010-9699-1 (2010).
60. Bloem, J., de Ruiter, P. C., Koopman, G. J., Lebbink, G. & Brussaard, L. Microbial numbers and activity in dried and rewetted arable soil under integrated and conventional management. *Soil. Biol. Biochem.* **24**, 655–665. https://doi.org/10.1016/0038-0717(92)90044-X (1992).
61. Fierer, N. & Schimel, J. P. A proposed mechanism for the pulse in carbon dioxide production commonly observed following the rapid rewetting of a dry soil. *Soil. Biol. Biochem.* **67**, 798–805. https://doi.org/10.2136/sssaj2003.0798 (2003).
62. Xiang, S. R., Doyle, A., Holden, P. A. & Schimel, J. P. Drying and rewetting effects on C and N mineralization and microbial activity in surface and subsurface California grassland soils. *Soil. Biol. Biochem.* **40**, 2281–2289. https://doi.org/10.1016/j.soilbio.2008.05.004 (2008).
63. Fierer, N. & Schimel, J. P. Effects of drying-rewetting frequency on soil carbon and nitrogen transformations. *Soil. Biol. Biochem.* **34**, 777–787. https://doi.org/10.1016/S0038-0717(02)00007-X (2002).
64. Sun, D. S. et al. Effects of organic amendment on soil aggregation and microbial community composition during drying-rewetting alternation. *Sci. Total Environ.* **574**, 735–743. https://doi.org/10.1016/j.scitotenv.2016.09.112 (2017).
65. Zhang, W. et al. Effects of drying and wetting cycles on the transformations of extraneous inorganic N to soil microbial residues. *Sci. Rep.* **7** https://doi.org/10.1038/s41598-017-09944-1 (2017).
66. Stedmon, C. A. et al. Photochemical production of ammonium and transformation of dissolved organic matter in the Baltic sea. *Mar. Chem.* **104**, 227–240. https://doi.org/10.1016/j.marchem.2006.11.005 (2007).
67. Levy-Booth, D. J., Prescott, C. E. & Grayston, S. J. Microbial functional genes involved in nitrogen fixation, nitrification and denitrification in forest ecosystems. *Soil. Biol. Biochem.* **75**, 11–25. https://doi.org/10.1016/j.soilbio.2014.03.021 (2014).
68. Kuypers, M. M. M., Marchant, H. K. & Kartal, B. The microbial nitrogen-cycling network. *Nat. Rev. Microbiol.* **16**, 263–276. https://doi.org/10.1038/nrmicro.2018.9 (2018).
69. Cuadros, J. Clay minerals interaction with microorganisms: A review. *Clay Min.* **52**, 235–261. https://doi.org/10.1180/claymin.2017.052.2.05 (2017).
70. Fuchs, G. in *Biology Prokaryotes* 110–160 (1998).
71. Nieder, R., Benbi, D. K. & Scherer, H. W. Fixation and defixation of ammonium in soils: A review. *Biol. Fertil. Soils*. **47**, 1–14. https://doi.org/10.1007/s00374-010-0506-4 (2011).
72. Herndon, E. M. et al. Iron (oxyhydr)oxides serve as phosphate traps in tundra and boreal peat soils. *J. Geophys. Res. Biogeosci.* **124**, 227–246. https://doi.org/10.1029/2018JG004776 (2019).
73. Nannipieri, P. et al. Soil enzymology: Classical and molecular approaches. *Biol. Fertil. Soils*. **48**, 743–762. https://doi.org/10.1007/s00374-012-0723-0 (2012).
74. Luo, G. W. et al. Soil carbon, nitrogen, and phosphorus cycling microbial populations and their resistance to global change depend on soil C:N:P stoichiometry. *mSystems* **5** (2020). https://doi.org/10.1128/mSystems.00162-20
75. Tian, Y. et al. Long-term soil warming decreases microbial phosphorus utilization by increasing abiotic phosphorus sorption and phosphorus losses. *Nat. Commun.* **14** https://doi.org/10.1038/s41467-023-36527-8 (2023).
76. Gao, L., Zhou, Z. Z., Reyes, A. V. & Guo, L. Yields and characterization of dissolved organic matter from different aged soils in Northern Alaska. *J. Geophys. Res.-Biogeosci.* **123**, 2035–2052. https://doi.org/10.1029/2018JG004408 (2018).
77. Mohinuzzaman, M. et al. Insights into solubility of soil humic substances and their fluorescence characterisation in three characteristic soils. *Sci. Total Environ.* **720**, 137395. https://doi.org/10.1016/j.scitotenv.2020.137395 (2020).
78. Zhang, J. et al. Isolation of dissolved organic matter from aqueous solution by precipitation with FeCl(3): Mechanisms and significance in environmental perspectives. *Sci. Rep.* **13**, 4531. https://doi.org/10.1038/s41598-023-31831-1 (2023).
79. Hemingway, J. D. et al. Mineral protection regulates long-term global preservation of natural organic carbon. *Nature* **570**, 228–231. https://doi.org/10.1038/s41586-019-1280-6 (2019).
80. Roth, V. N. et al. Persistence of dissolved organic matter explained by molecular changes during its passage through soil. *Nat. Geosci.* **12**, 755–761. https://doi.org/10.1038/s41561-019-0417-4 (2019).
81. Mostofa, K. M. G., Yoshioka, T., Mottaleb, M. A. & Vione, D. *Photobiogeochem. Organ. Matter Principles Pract. Water Environ.* (Springer, 2013).
82. Yang, X. et al. New insights into mechanisms of sunlight- and dark-mediated high-temperature accelerated diurnal production-degradation of fluorescent DOM in lake waters. *Sci. Total Environ.* **760**, 143377. https://doi.org/10.1016/j.scitotenv.2020.143377 (2021).
83. Rousk, J. & Jones, D. L. Loss of low molecular weight dissolved organic carbon (DOC) and nitrogen (DON) in H2O and 0.5 M K2SO4 soil extracts. *Soil. Biol. Biochem.* **42**, 2331–2335. https://doi.org/10.1016/j.soilbio.2010.08.017 (2010).
84. Mostofa, K. M. G., Yoshioka, T., Konohira, E. & Tanoue, E. Photodegradation of fluorescent dissolved organic matter in river waters. *Geochem. J.* **41**, 323–331. https://doi.org/10.2343/geochemj.41.323 (2007).
85. Fang, C., Smith, P., Moncrieff, J. B. & Smith, J. U. Similar response of labile and resistant soil organic matter pools to changes in temperature. *Nature* **433**, 57–59. https://doi.org/10.1038/nature03138 (2005).

86. Smith, H. J. et al. Microbial formation of labile organic carbon in Antarctic glacial environments. *Nat. Geosci.* **10**, 356–359. https://doi.org/10.1038/NGEO2925 (2017).
87. He, T., Sun, Y. B., Gray, J. & Gu, Y. Provenance of Fe in Chinese deserts: Evidence from the geochemistry and mineralogy of soil particles. *Catena* **198** https://doi.org/10.1016/j.catena.2020.105053 (2021).
88. Kneip, C., Lockhart, P. J., Voss, C. & Maier, U. G. Nitrogen fixation in eukaryotes—new models for symbiosis. *BMC Evol. Biol.* **7**, 55–55 (2007).
89. Levicán, G., Ugalde, J. A., Ehrenfeld, N., Maass, A. & Parada, P. Comparative genomic analysis of carbon and nitrogen assimilation mechanisms in three Indigenous bioleaching bacteria: Predictions and validations. *BMC Genom.* **9**, 581. https://doi.org/10.1186/1471-2164-9-581 (2008).
90. Malik, A. A. et al. Land use driven change in soil pH affects microbial carbon cycling processes. *Nat. Commun.* **9** https://doi.org/10.1038/s41467-018-05980-1 (2018).
91. Fierer, N. & Jackson, R. B. The diversity and biogeography of soil bacterial communities. *Proc. Natl. Acad. Sci. U.S.A.* **103**, 626–631 (2006). https://doi.org/10.1073/pnas.0507535103
92. Soti, P. G., Jayachandran, K., Koptur, S. & Volin, J. C. Effect of soil pH on growth, nutrient uptake, and mycorrhizal colonization in exotic invasive lygodium microphyllum. *Plant. Ecol.* **216**, 989–998. https://doi.org/10.1007/s11258-015-0484-6 (2015).
93. Yang, X. et al. Solubility characteristics of soil humic substances as a function of pH: Mechanisms and biogeochemical perspectives. Biogeosciences (accepted).
94. Aciego Pietri, J. C. & Brookes, P. C. Nitrogen mineralisation along a pH gradient of a silty loam UK soil. *Soil. Biol. Biochem.* **40**, 797–802. https://doi.org/10.1016/j.soilbio.2007.10.014 (2008).
95. Kemmitt, S. J., Wright, D., Goulding, K. W. T. & Jones, D. L. pH regulation of carbon and nitrogen dynamics in two agricultural soils. *Soil. Biol. Biochem.* **38**, 898–911. https://doi.org/10.1016/j.soilbio.2005.08.006 (2006).
96. Yang, X. et al. Mineral States and sequestration processes involving soil biogenic components in various soils and desert sands of inner Mongolia. *Sci. Rep.* **14**, 28530. https://doi.org/10.1038/s41598-024-80004-1 (2024).
97. Pietikainen, J., Pettersson, M. & Baath, E. Comparison of temperature effects on soil respiration and bacterial and fungal growth rates. *FEMS Microbiol. Ecol.* **52**, 49–58. https://doi.org/10.1016/j.femsec.2004.10.002 (2005).
98. Gilbert, B., Lu, G. P. & Kim, C. S. Stable cluster formation in aqueous suspensions of iron oxyhydroxide nanoparticles. *J. Colloid Interface Sci.* **313**, 152–159. https://doi.org/10.1016/j.jcis.2007.04.038 (2007).
99. Yang, D. H. et al. Saline-alkali stress reduces soil bacterial community diversity and soil enzyme activities. *Ecotoxicology* **31**, 1356–1368. https://doi.org/10.1007/s10646-022-02595-7 (2022).
100. Zhang, Z. et al. A review of sulfate-reducing bacteria: Metabolism, influencing factors and application in wastewater treatment. *J. Clean. Prod.* **376** https://doi.org/10.1016/j.jclepro.2022.134109 (2022).
101. Hilton, R. G. & West, A. J. Mountains, erosion and the carbon cycle. *Nat. Rev. Earth Environ.* **1**, 284–299. https://doi.org/10.1038/s43017-020-0058-6 (2020).
102. Zamanian, K., Zhou, J. B. & Kuzyakov, Y. Soil carbonates: The unaccounted, irrecoverable carbon source. *GEODERMA* **384** https://doi.org/10.1016/j.geoderma.2020.114817 (2021).
103. Kelly, B. et al. Sulfur sequestration promotes multicellularity during nutrient limitation. *Nature* **591**, 471–476. https://doi.org/10.1038/s41586-021-03270-3 (2021).
104. Jordaan, K. et al. Hydrogen-oxidizing bacteria are abundant in desert soils and strongly stimulated by hydration. *mSystems* **5** https://doi.org/10.1128/mSystems.01131-20 (2020).
105. Lange, O. L., Belnap, J. & Reichenberger, H. Photosynthesis of the cyanobacterial soil-crust lichen Collema tenax from arid lands in Southern Utah, USA: Role of water content on light and temperature responses of CO_2 exchange. *Funct. Ecol.* **12**, 195–202 (1998).
106. Steven, B., Belnap, J. & Kuske, C. R. Chronic physical disturbance substantially alters the response of biological soil crusts to a wetting pulse, as characterized by metatranscriptomic sequencing. *Front. Microbiol.* **9** https://doi.org/10.3389/fmicb.2018.02382 (2018).
107. Bay, S., Ferrari, B. & Greening, C. Life without water: How do bacteria generate biomass in desert ecosystems? *Microbiol. Aust*. **39**, 28–32. https://doi.org/10.1071/ma18008 (2018).
108. Georgiou, C. D. et al. Evidence for photochemical production of reactive oxygen species in desert soils. *Nat. Commun.* **6** https://doi.org/10.1038/ncomms8100 (2015).
109. Yu, G. H. et al. Fungal nanophase particles catalyze iron transformation for oxidative stress removal and iron acquisition. *Curr. Biol.* **30**, 2943–. https://doi.org/10.1016/j.cub.2020.05.058 (2020).
110. Lehmann, J. & Kleber, M. The contentious nature of soil organic matter. *Nature* **528**, 60–68. https://doi.org/10.1038/nature16069 (2015).

Acknowledgements

This study was supported by the National Natural Science Foundation of China (Grant Nos. U1612441 and 42230509), the Ministry of Science and Technology of China (Grant Nos. 2019YFC1804400) and also by the Key Construction Program of the National "985" Project, Tianjin University, China.

Author contributions

Conceptualization, Supervision (K.M.G.M., S.L.L.), writing—original draft (K.M.G.M., N.S., J.Z.), investigation and formal analysis (X.G., J.Z.), validation (X.G., J.Z., K.M.G.M., W.Z., C.Q.L, N.S., G.S.S., D.V., J.Y., Y.L., M.M., L.L.L., SLL), writing—review & editing (C.Q.L., G.S.S., D.V., S.L.L.), PARAFAC analysis (J.Y.).

Declarations

Competing interests

The authors declare no competing interests.

Additional information

Supplementary Information The online version contains supplementary material available at https://doi.org/10.1038/s41598-025-94920-3.

Correspondence and requests for materials should be addressed to K.M.G.M. or S.-L.L.

Reprints and permissions information is available at www.nature.com/reprints.

Publisher's note Springer Nature remains neutral with regard to jurisdictional claims in published maps and institutional affiliations.

Open Access This article is licensed under a Creative Commons Attribution-NonCommercial-NoDerivatives 4.0 International License, which permits any non-commercial use, sharing, distribution and reproduction in any medium or format, as long as you give appropriate credit to the original author(s) and the source, provide a link to the Creative Commons licence, and indicate if you modified the licensed material. You do not have permission under this licence to share adapted material derived from this article or parts of it. The images or other third party material in this article are included in the article's Creative Commons licence, unless indicated otherwise in a credit line to the material. If material is not included in the article's Creative Commons licence and your intended use is not permitted by statutory regulation or exceeds the permitted use, you will need to obtain permission directly from the copyright holder. To view a copy of this licence, visit http://creativecommons.org/licenses/by-nc-nd/4.0/.

© The Author(s) 2025